Optimal Trajectories for Nonholonomic Mobile Robots

P. Souères J.D. Boissonnat

This is the third chapter of the book:

Robot Motion Planning and Control
Jean-Paul Laumond (Editor)

Laboratoire d'Analye et d'Architecture des Systèmes
Centre National de la Recherche Scientifique
LAAS report 97438

Previoulsy published as:
Lectures Notes in Control and Information Sciences 229.
Springer, ISBN 3-540-76219-1, 1998, 343p.

Optimal Trajectories for Nonholonomic Mobile Robots

P. Souères[1] and J.-D. Boissonnat[2]

[1] LAAS - CNRS, Toulouse
[2] INRIA, Sophia Antipolis

1 Introduction

From a kinematic point of view, the main characteristic of wheeled robots is the nonholonomic rolling without slipping constraint of the wheels on the floor, which forces the vehicle to move tangentially to its main axis. This reduction of the set of accessible velocities at each time makes the path planning problem particularly difficult. Among the different methods devoted to solve this problem we want to focus on those based on the characterization of shortest paths or time-optimal paths, which turn out to be particularly efficient. Indeed, the knowledge of an optimal strategy for linking any two configurations allows to determine simple canonical paths and provides a topological modeling of the problem by defining a new "distance function" taking into account the nonholonomic nature of the system. Unfortunately, the characterization of optimal paths for this class of nonlinear systems is not an easy task.

The works presented in this chapter are based on Pontryagin's Maximum Principle (PMP) which constitutes a generalization of Lagrange's problem of the calculus of variation. PMP is a local reasoning based on the comparison of trajectories corresponding to infinitesimally close control laws. It provides necessary conditions for paths to be optimal. Nevertheless, though this condition brings a very strong information about the nature of optimal paths for certain kind of systems, it turns out to be insufficient to solve the optimal control problems we are interested on.

Indeed, on the one hand the nonlinear nature of these systems makes the adjoint differential equations seldom integrable. Therefore, in the most part of cases, the necessary condition of PMP only provides a local characterization of optimal trajectories. On the other hand, the study of such systems has shown that the set of accessible configurations at each time, is neither smooth nor convex. More precisely, it appears that the boundary of this set is made up by several smooth pieces corresponding to the propagation of several wave fronts. This is due at one and the same time to the difficulty of moving sideways and the natural symmetries of the problem.

For these latter reasons, the local nature of PMP cannot provide a tool to compare the cost of trajectories corresponding to different wave fronts. Therefore, this local information needs to be completed with a global study.

By combining these two approaches it is sometimes possible to get a better characterization of the solution. In this way, a first interesting result is the determination of a sufficient family of trajectories i.e. a family of trajectories containing an optimal solution for linking any two configurations. Whenever this family is small enough and sufficiently well specified it is possible to compare the cost of trajectories by means of a numerical method. Nevertheless, the ultimate goal one wants to reach is to achieve the determination of an optimal control law for steering the representative point from any point of the phase space to a given target set, i.e. to solve the synthesis problem.

Four works are presented in this chapter, devoted to the search of optimal paths for various models of wheeled robots. These problems are stated in the free phase space i.e. without obstacles. We have been able to solve the synthesis problem for only two of these models. The two other works provide an incomplete characterization of optimal solutions, bringing to the fore various kind of difficulties that can be encountered in studying such problems.

The paper is organized as follows: The models of wheeled robots and their related optimization problems are presented in section 2. The third section constitutes a survey of the definitions and results from optimal control theory which have been useful for these different works: Fillipov's existence theorem, Pontryagin's Maximum Principle (PMP) and Boltianskii's sufficient optimality condition. In particular, we give a geometric description of PMP in order to point out the local nature of this reasoning. The last four sections present successively the works related to each model.

2 Models and optimization problems

The aim of the works presented in this chapter is to characterize optimal trajectories verifying the nonholonomic constraints of mobile robots. Therefore, in order to get the simplest expression of the problem, we consider mathematical models defined upon the kinematic constraints inherent in these wheeled vehicles, without taking into account their dynamics. Classically, these models are described by differential autonomous[1] systems such as:

$$\frac{dx^i}{dt} = f^i(x^1, x^2, \dots, x^n, u^1, u^2, \dots, u^m) \tag{1}$$

[1] The function f does not depend explicitly on time.

where the x^i characterize the robot's coordinates in the phase space and the control parameters u^i express the existence of "rudders" such as the steering wheel or the brake-accelerator function. Once the control parameters are defined as time-varying functions $u_j = u_j(t), j = 1, \ldots, m$, the corresponding trajectory solution of (1) is uniquely determined by the choice of initial conditions $x^i(t_0) = x_0^i, i = 1, \ldots, n$.

2.1 Dubins' and Reeds-Shepp's car

The model of a car-like robot considered here, describes the two principal kinematic constraints of an usual car. The first one is the rolling without slipping constraint which obliges the vehicle to move tangentially to its main axis. The second constraint is due to the bound on the turning wheels' angle and prevents the car from moving on trajectories whose radius of curvature is lower than a given threshold R. A configuration of the car is represented by a triple $(x, y, \theta) \in \mathbf{R}^2 \times S^1$, where (x, y) are the coordinates of a reference point of the robot with respect to a Cartesian frame, and θ is the angle between the positive x-axis and the robot's main axis, see figure (1). With this modeling, the rolling without slipping constraint is expressed by the following equation:

$$\dot{y}\cos\theta - \dot{x}\sin\theta = 0$$

For our purpose, the direction of front wheels is not relevant, we only need to consider that the bound on the angle of steer ϕ induces an upper bound on the trajectories' curvature.

Therefore, the kinematics of the vehicle is described by the differential system (2) involving two control parameters u_1 and u_2 which represent respectively the algebraic value of the linear and angular velocities.

$$\begin{pmatrix} \dot{x} \\ \dot{y} \\ \dot{\theta} \end{pmatrix} = \begin{pmatrix} \cos\theta \\ \sin\theta \\ 0 \end{pmatrix} u_1 + \begin{pmatrix} 0 \\ 0 \\ \frac{1}{R} \end{pmatrix} u_2 \tag{2}$$

This kinematic model was introduced by Dubins in 1957 [16] who set the problem of characterizing the shortest paths for a particle moving forward in the plane with a constant linear velocity ($u_1 = k$). Later, Reeds and Shepp [31] considered the same problem, when backwards motions are allowed ($|u_1| = k$). In both cases, as the modulus of the linear velocity keeps constant, the shortest path problem is equivalent to the minimum-time problem.

In the sequel without lost of generality we will fix the value of the constants: $R = 1$ and $k = 1$.

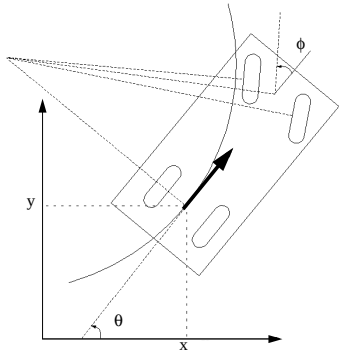

Fig. 1. The car-like model

2.2 Dubins' car with inertial angular velocity

As we will see later in detail, the optimal solutions of Dubins' problem are sequences of line segments and arcs of circle of minimal radius. Therefore, the curvature along the trajectory does not vary continuously. As a consequence, any real robot following such a trajectory would be constrained to stop at each curvature discontinuity.

In order to avoid this problem, Boissonnat, Cerezo and Leblond [3] have proposed a dynamic extension of Dubins' problem by controlling the angular acceleration of the car instead of its angular velocity. The curvature κ is now considered as a new phase variable, and the angular acceleration v is bounded inside a compact interval $[-B, B]$.

$$\begin{pmatrix} \dot{x} \\ \dot{y} \\ \dot{\theta} \\ \dot{\kappa} \end{pmatrix} = \begin{pmatrix} \cos\theta \\ \sin\theta \\ \kappa \\ 0 \end{pmatrix} + \begin{pmatrix} 0 \\ 0 \\ 0 \\ 1 \end{pmatrix} v \tag{3}$$

For this problem, as for Dubins problem, minimizing the time comes to the same as minimizing the length.

2.3 The robot HILARE

The locomotion system of Hilare the robot of LAAS-CNRS consists of two parallel independently driven wheels and four slave castors. The velocities v_r and v_l of the right and left driven wheels are considered as phase variables and

a configuration of the robot is a 5-uple (x, y, θ, v_r, v_l). The accelerations a_r and a_l of each driven wheel are the inputs to the following control system:

$$\begin{pmatrix} \dot{x} \\ \dot{y} \\ \dot{\theta} \\ \dot{v}_r \\ \dot{v}_l \end{pmatrix} = \begin{pmatrix} \frac{v_r+v_l}{2}\cos\theta \\ \frac{v_r+v_l}{2}\sin\theta \\ \frac{v_r-v_l}{d} \\ 0 \\ 0 \end{pmatrix} + \begin{pmatrix} 0 \\ 0 \\ 0 \\ 1 \\ 0 \end{pmatrix} a_r + \begin{pmatrix} 0 \\ 0 \\ 0 \\ 0 \\ 1 \end{pmatrix} a_l \tag{4}$$

where $a_r, a_l \in [-a_{\max}, a_{\max}]$, and $d > 0$ is the distance between the wheels. In this case the trajectories' curvature is not bounded and the robot can turn about its reference point.

For this model, we consider the problem of characterizing minimum-time trajectories linking any pair of configurations where the robot is at rest i.e verifying $v_r = v_l = 0$.

3 Some results from Optimal Control Theory

3.1 Definitions

Let us now define the notion of dynamical system in a more precise way. Let M be a n-dimensional manifold, and U a subspace of $\mathbf{R}^m$. We study the motion of a representative point $x(t) = (x^1(t), \ldots, x^n(t))$ in the phase space M, depending on the control law $u(t) = (u^1(t), \ldots, u^m(t))$ taking its values in the control set U. In this chapter, we define the set of admissible control laws as the class of measurable functions from the real time interval $[t_0, t_1]$ to U. As we said in the previous section, the motion of the representative point is described by an autonomous differential system of the form:

$$\frac{dx^i}{dt} = f^i(x(t), u(t)) \;\; i = 1, \ldots, n \tag{5}$$

We consider now a function $L(x, u)$ defined on the product $M \times U$, continuously differentiable with respect to its arguments. Given any two points x_0 and x_1 in the phase space M, we want to characterize, among all the control laws steering the representative point from x^0 to x^1, one (if exists) minimizing the functional:

$$J = \int_{t_0}^{t_1} L(x(\tau, u), u(\tau))d\tau$$

Remark 1. *The initial and final time t_0 and t_1 are not fixed* a priori*, they depend on the control law $u(t)$.*

Definition 1. *Two trajectories are said to be* equivalent *for transferring the representative point from x_0 to x_1 if they their respective costs are equal.*

In the sequel we restrict our study to the minimum-time problem. In this case $L(x, u) \equiv 1$ and $J = t_1 - t_0$.

In chapter 1 it has been shown that the models described in the previous section are fully controllable in their phase space M, i.e. given any two configurations x_0 and x_1 in M there always exists a trajectory, solution of (5), linking x_0 to x_1. Nevertheless it is not possible to deduce from this result whether a minimum-time feasible path from x_0 to x_1 exists or not. This last question constitutes an important field of interest of optimal control theory (cf [13] for a detailed survey). In particular, there exist some general theorems due to Fillipov, ensuring the existence of optimal paths under some convexity hypotheses. The next subsection presents two theorems that will be sufficient for our purpose.

3.2 Existence of optimal paths

Let M be an open subset of $\mathbf{R}^n$ or a n-dimensional smooth manifold, and U a subset of $\mathbf{R}^m$.

Theorem 1. (Fillipov's general theorem for minimum-time problems)

Let x_0, x_1 be two points in M. Under the following hypotheses there exists a time-optimal trajectory solution of (5) linking x_0 to x_1.

H_1 - f is a continuous function of t, u, x and a continuously differentiable function of x.

H_2 - the control set U is a **compact** subset of $\mathbf{R}^m$. Furthermore, when u varies in U, the image set F(t,x) described by $f(x(t), u(t))$ is **convex** for all $t, x \in [t_0, t_1] \times M$.

H_3 - there exists a constant C such that for all $(t, x) \in [t_0, t_1] \times M$:

$$< x, f(t, x, u) > \ \leq \ C\ (1 + |x|^2)$$

H_4 - there exists an admissible trajectory from x_0 to x_1

Remark 2. - *The hypothesis H_3 prevents from a finite escape time of the phase variable x for any admissible control law $u(.)$.*

When f is a linear function of the control parameters u_i of the form:

$$f(x, u) = g_1(x)\ u_1 + \ldots + g_m(x)\ u_m, \tag{6}$$

there exists a simpler version of this result given by the next theorem.

Theorem 2. Let x_0 and x_1 be two points in M. Under the following hypotheses there exists an optimal trajectory solution of (6) linking x_0 to x_1.

H_1 - the g_i are locally lipschitzian functions of x.
H_2 - the control set U is a **compact convex** subset of $\mathbf{R}^m$
H_3 - there exists an admissible trajectory from x_0 to x_1
H_4 - The system is complete, in the sense that given any point $x_0 \in M$, and any admissible control law $u(.)$, there exists a corresponding trajectory $x(t, u)$ defined on the whole time interval $[t_0, t_1]$ and verifying $x(t_0, u) = x_0$.

3.3 Necessary conditions: Pontryagin's Maximum Principle

Pontryagin's Maximum Principle (PMP) provides a method for studying variational problems in a more general way than the classical calculus of variation does. Indeed, when the control set U is a closed subset of $\mathbf{R}^m$, the Weierstrass' condition characterizing the minimum of the cost functional is no more valid. The case of closed control set is yet the most interesting one for modeling concrete optimal control problems. PMP provides a necessary condition for the solutions of a general control systems to be optimal for various kind of cost functional. In this chapter we restrict our statement of PMP to minimum-time problems.

We consider the dynamical system (5) where x belongs to an open subset $\Omega \subset \mathbf{R}^n$ or a smooth n-dimensional manifold M.

Definition 2.

- Let ψ be a n-dimensional real vector, we define the Hamiltonian *of system (5) as the $\mathbf{R}$-valued function H defined on the set $\mathbf{R}^n_* \times \Omega \times U$ by:*

$$H(\psi, x, u) =< \psi, f(x, u) > \tag{7}$$

where $\mathbf{R}^n_* = \mathbf{R}^n \setminus \{0\}$, and $< ., . >$ is the usual inner product of $\mathbf{R}^n$.

- If $u(.) : [t_0, t_1] \to U$ is an admissible control law and $x(t) : [t_0, t_1] \to \Omega$ the corresponding trajectory, we define the adjoint vector *for the pair (x, u) as the absolutely continuous vector function ψ defined on $[t_0, t_1]$, taking its values in $\mathbf{R}^n_*$ which verifies the following* adjoint equation *at each time $t \in [t_0, t_1]$:*

$$\dot{\psi}(t) = -\frac{\partial H}{\partial x}(\psi(t), x(t), u(t)) \tag{8}$$

Remark 3. *As H is a linear function of ψ, $\dot{\psi}$ is also a linear function of ψ. Therefore, either $\psi(t) \neq 0 \ \forall t \in [t_0, t_1]$, or $\psi(t) \equiv 0$ on the whole interval $[t_0, t_1]$; in the latter case, the vector ψ is said to be* trivial.

Theorem 3. (Pontryagin's Maximum Principle) Let $u(.)$ be an admissible control law defined on the closed interval $[t_0, t_1]$ and $x(t)$ the corresponding trajectory. A necessary condition for $x(t)$ to be time-optimal is that there exists an absolutely continuous non trivial adjoint vector $\psi(t)$ associated to the pair (x, y), and a constant $\psi_0 \leq 0$ such that $\forall t \in [t_0, t_1]$:

$$H(\psi(t), x(t), u(t)) = \max_{v \in U}(H(\psi(t), x(t), v(t)) = -\psi_0 \tag{9}$$

Definition 3.

- A control law $u(t)$ satisfying the necessary condition of PMP is called an extremal *control law. Let $x(t, u)$ be the corresponding trajectory and $\psi(t)$ the adjoint vector corresponding to the pair (x, u); the triple (x, u, ψ) is also called* extremal.

- To study the variations of the Hamiltonian $H = \Sigma_i\ \dot{x}_i(t)\ \psi_i(t)$ one can rewrite H in the form: $H = \Sigma_i \phi_i(t)\ u_i(t)$ where the ϕ_i, called switching functions *determine the sign changes of u_i.*

Sometimes the maximization of the function H does not define a unique control law. In that case the corresponding control is called *singular*:

Definition 4. *A control $u(t)$ is* singular *if there exists a nonempty subset $W \subset U$ and a non empty interval $I \subset [t_0, t_1]$ such that $\forall t \in I,\ \forall w(t) \in W$:*

$$H(\psi(t), x(t), u(t)) = H(\psi(t), x(t), w(t))$$

In particular, when a switching function vanishes over a non empty open interval of time, the corresponding control law comes singular. In that case, all the derivatives of the switching function also vanish on this time interval, providing a sequence of equations. From these relations, it is sometimes possible to characterize the value of the corresponding singular control.

The following theorem allows to compute easily those derivatives in terms of Lie brackets.

Theorem 4. Let Z be a smooth vector field defined on the manifold M and (x, u, ψ) an extremal triple for the system (6).

The derivative of the function $\phi_Z(.) :\ t \longrightarrow\ < \psi(t), Z(x(t)) >$ is defined by:

$$\dot{\phi}_Z(t) = \sum_{i=1}^{r} < \psi, [g_i, Z]x(t) > .u_i$$

Let us now define the notion of reachable set:

Definition 5. - *We denote by* $\mathcal{R}(x_0, T)$*, and we call* set of accessibility from x_0 in time T*, the set of points* $x \in M$ *such that there exists a trajectory solution of (5) transferring the representative point from* x_0 *to* x *in a time* $t \leq T$*.*

- *The set* $\mathcal{R}(x_0) = \bigcup_{0 \leq T \leq \infty} \mathcal{R}(x_0, T)$ *is called* set of accessibility from x_0.

When the system is fully controllable (controllable from any point) the set of accessibility $\mathcal{R}(x_0)$ from any point x_0 is equal to the whole manifold M. Otherwise, $\mathcal{R}(x_0)$ is restricted to a closed subset of M. In this latter case there exists another version of PMP.

Theorem 5. (PMP for boundary trajectories) Let $u(.) : [t_0, t_1] \rightarrow U$ be an admissible control law, and $x(t)$ the corresponding trajectory transferring the representative point from x_0 to a point x_1 belonging to the boundary $\partial\mathcal{R}(x_0)$ of the set $\mathcal{R}(x_0)$. A necessary condition for the trajectory $x(t, u)$ to be time-optimal, is that there exists a non-trivial adjoint vector ψ verifying relation (9) with $\psi_0 = 0$

Definition 6. *An extremal triple* (x, u, ψ) *such that* $\psi_0 = 0$ *is called* abnormal .

Commentary about PMP: It is often difficult to extract a precise information from PMP. Indeed, it is seldom possible to integrate the adjoint equations or to characterize the singular control laws. Furthermore, one can never be sure to have got all the information it was possible to deduce from PMP. Sometimes, the information obtained is very poor, and the set of potential solutions too large.

An interesting expected result is the characterization of a *sufficient family* of trajectory i.e. a family of trajectory containing an optimal solution for linking any pair of points $(x_0, x_1) \in M$. When this family is small enough, and sufficiently well specified the optimal path may be selected by means of a numerical test.

Nevertheless, the ultimate goal one wants to reach is the exact characterization of the optimal control law allowing to steer the point between any two states of M. However, though it is possible to deduce directly the structure of minimum-time trajectories from PMP for linear systems, the local information is generally insufficient to conclude the study in the case of nonlinear systems. As we will see in the sequel, it is yet sometimes possible to complete the local information provided by PMP by making a geometric study of the problem. When the characterization of optimal path is complete, a synthetic way of representing the solution is to describe a network of optimal paths linking any point of the state space to a given target point. The following definition due to Pontryagin states this concept in a more precise way.

Definition 7. *For a given optimization problem, we call* synthesis function*, a function $v(x)$ (if it exists) defined in the phase space M and taking its values in the control set U, such that the solutions of the equation:*

$$\frac{dx}{dt} = f(x, v(x))$$

are optimal trajectories linking any point of M to the origin. The problem of characterizing a synthesis function is called synthesis problem *and the corresponding network of optimal paths is called a* synthesis of optimal paths *on M.*

A geometric illustration of PMP: In the statement of PMP, optimal control laws are specified by the maximization of the inner product of two vectors. In the rest of this section, drawing our inspiration from a work by H. Halkin [21], we try to give a geometric interpretation of this idea by pointing out the analogy between optimal control and propagation phenomena. In this, we want to focus on the local character of PMP in order to point out its insufficiency for achieving the characterization of shortest paths for nonholonomic problems. This remark emphasizes the necessity to complete the local reasoning by making use of global arguments.

At the basis of the mathematical theory of optimal process stands the *principle of optimal evolution* which can be stated as follows:

" If $x(t, u)$ is an optimal trajectory starting from x_0 at time t_0, then at each time $t \geq t_0$ the representative point must belong to the boundary $\partial\mathcal{R}(x_0, t)$ of the set $\mathcal{R}(x_0, t)$ "

For some physical propagation phenomena, such as the isotropic propagation of a punctual perturbation on the surface of water, the wavefront associated with the propagation coincides at each time with the boundary of the set of accessibility. Let us consider first the simple propagation of a signal starting at a point x_0 such that the set of accessibility $\mathcal{R}(x_0, t)$ at each time t be smooth and convex with a unique tangent hyperplane defined at each boundary point.

As in geometrical optics, at each time t and at each boundary point x, we can define the wavefront velocity as a nonzero vector $\boldsymbol{V}(x, t) = V(x, t)\ \boldsymbol{k}(x, t)$ where $V(x, t)$ is a $\mathbf{R}$-valued function of x and t, and $\boldsymbol{k}(x, t)$ a unit vector outward normal to the hyperplane tangent to $\mathcal{R}(x_0, t)$ at x. Now, according to the principle of optimal evolution, if $x(t, u)$ is an optimal trajectory starting at x_0, the following two conditions must be verified:

- For any admissible motion, corresponding to a control $w(t)$, the projection of the representative point velocity $\dot{x}(t, w) = f(x, w)$ on the line passing through $x(t, w)$ and whose direction is given by the vector $k(x, t)$, is at most equal to the wavefront speed $V(x, t)$.

$$< f(x(t), w(t)), k(x,t) > \leq \ V(x,t) \tag{10}$$

– With the optimal control u, the representative point must keep up with the wavefront $\partial\mathcal{R}(x_0,t)$ i.e. the projection of the representative point's velocity on the normal vector $k(x,t)$ determines the wavefront velocity.

$$< f(x(t), u(t)), k(x,t) > = \ V(x,t) \tag{11}$$

Now, by identifying the adjoint vector $\psi(x,t)$ with $V(x,t)$ we can make a link between relations (10, 11) and the maximization of the Hamiltonian defined by (9).

Though this analogy with propagation phenomena provides a good geometric meaning of this principle of optimization, it is not easy to generalize this idea to any dynamical system. Indeed, for a general system, the set $\mathcal{R}(x_0,t)$ is not necessarily convex and its boundaries are not necessarily smooth. In order to get a geometric meaning of Pontryagin's result in the general case, it is convenient to consider the cost functional J as a new phase variable x^0, and to manage our reasoning in the augmented phase space $\mathbf{R} \times \Omega \subset \mathbf{R}^{n+1}$. Therefore, at each time, the velocity vector of the representative point $X = (x^0, x) = (x^0, x^1, \ldots .x^n)$ corresponding to the control law $u(.)$ is given by $\hat{f}(X,u) = (L(x,u), f^1(x,u), \ldots , f^n(x,u))$. With this representation the optimization problem becomes:

"Let $\mathcal{D}$ be the line passing through $(0, x_1)$ parallel to the x^0-axis. Among all the trajectories starting at $X_0 = (0, x_0)$ and reaching $\mathcal{D}$, find one, if exists, which minimizes the first coordinate x^0 of the point of intersection $X_1 = (x^0, x_1)$ with $\mathcal{D}$."

As before we define the set of accessibility $\mathcal{R}(X_0,t)$ from X_0 in the augmented phase space. Now, it is easy to prove that any optimal path must verify the principle of optimality. Indeed, if the point X_1 of $\mathcal{D}$, reached at time t_1 with control u, lies in the interior of $\mathcal{R}(X_0,t_1)$, there exists necessarily a neighbourhood of X_1 containing a point of $\mathcal{D}$ located "under" X_1 and the control u cannot be optimal. Furthermore, due to the smoothness properties of the function $\hat{f}$, if the point X, reached at time $\tau \in [t_0, t_1]$ with u, is in the interior of $\mathcal{R}(X_0,\tau)$, then for all $t \geq \tau$ the representative point will belong to the interior of $\mathcal{R}(X_0,t)$.

Now, let $X(t,u)$ be a trajectory starting at X_0, optimal for reaching the line $\mathcal{D}$. In order to use the same reasoning as before, Pontryagin's *et al* have proven that it is still possible to construct a separating hyperplane by using the following idea: By replacing $u(.)$ by other admissible control laws on "small" time intervals they define new admissible control laws $\tilde{u}$ infinitesimaly close to u. Then, a part of their proof consists in showing that the set of point $X(t,\tilde{u})$

reached at each time t by the "perturbed" trajectories constitutes a convex cone $\mathcal{C}$ with vertex $X(t,u)$, contained in $\mathcal{R}(X_0,t)$. This cone locally approximates the set $\mathcal{R}(X_0,t)$ and does not contain the half-line $\mathcal{D}^-$ starting at $X(t,u)$ in the direction of the decreasing x^0. It is then possible to find an hyperplane $\mathcal{H}$ tangent to $\mathcal{C}$ at $X(t,u)$, separating $\mathcal{C}$ and the half-line $\mathcal{D}^-$, and containing the vector $\hat{f}(t,u)$. Now, the reasoning is the same as before; the adjoint vector $\hat{\psi} = (\psi^0, \psi^1, \ldots, \psi^n)$ is defined, up to a multiplicative constant, as the vector outward orthogonal to this hyperplane at each time. Following the principle of optimal evolution, the projection of the vector $\hat{f}(t,u)$ on the line parallel to $\hat{\psi}(t)$, passing through $x(t,u)$, must be maximal for the control u.

The case of nonholonomic systems: As we will see later, the nonholonomic rolling without slipping constraint, characteristic of wheeled robots, makes their displacement anisotropic. Indeed, although forwards motion can be easily performed, moving sideways may require numerous manoeuvres. For this reason, and due to the symmetry properties of such systems, the set of accessibility (in time) is generally not convex and its boundary does not coincide everywhere with the wavefront associated with the propagation. Instead of this, we will show later that the boundary is made up by the propagation of several intersecting wavefronts. Therefore, a local method like PMP, based on the comparison of very close control laws cannot be a sufficient tool to compare the cost of trajectories corresponding to different wavefronts. This very important point will be illustrated in section 4 through the construction of a synthesis of optimal paths for the Reeds-Shepp car.

So far, we only have stated necessary conditions for trajectories to be optimal. We now present a theorem by V. Boltyanskii which states sufficient optimality conditions under very strong hypotheses.

3.4 Boltyanskii's sufficient conditions

In this section we recall Boltianskii's definition of a regular synthesis as stated in [4]. This concept is based on the definition of a *piecewise-smooth set.*

Let M be a n-dimensional vector space, and Ω an open subset of M. Let E an s-dimensional vector space ($s \leq n$) and $K \subset E$ a bounded, s-dimensional convex polyhedron. Assume that in a certain open set of E containing K are given n continuously differentiable functions $\varphi^i(\xi^1, \xi^2, \ldots, \xi^s)$, $(i = 1, 2, \ldots, n)$ such that the rank of the matrix of partial derivatives $(\frac{\partial \varphi^i}{\partial \xi^j})$, $(i = 1, 2, \ldots, n)$, $(j = 1, 2, \ldots, s)$ be equal to s at every point $\xi \in K$.

Definition 8. - *If the smooth vector mapping* $\varphi = (\varphi^1, \varphi^2, \ldots, \varphi^n)$ *from* K *to* M *is injective, the image* $L = \varphi(K)$ *is called a s-dimensional* curvilinear polyhedron *in* M.

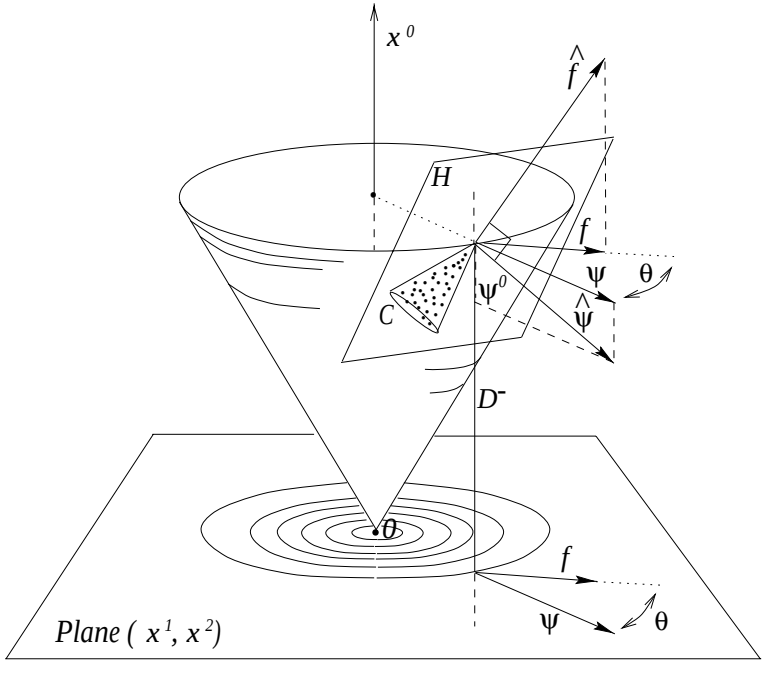

Fig. 2. Hyperplane $\mathcal{H}$ separating the half-line $\mathcal{D}^-$ and the convex cone $\mathcal{C}$.

- Any set $\mathcal{X} \subset \Omega$ which is the union of a finite or countable number of curvilinear ployhedra, such that only a finite number of these polyhedra intersect every closed bounded set lying in Ω, will be called a piecewise-smooth *set in Ω. The dimension of this set will be the highest dimension of polyhedra involved in the construction.*

Remark 4. *It has been proven in [12] that any non-singular smooth surface of dimension less than n, closed in Ω, can be decomposed in a finite number of curvilinear polyhedra. Therefore, such a surface is is a piecewise-smooth set in Ω.*

Now let us state the problem: In the n-dimensional space M, we consider the following system:

$$\frac{dx^i}{dt} = f^i(x^1, \ldots, x^n, u) \quad i = 1, \ldots, n \tag{12}$$

where the control $u = (u_1, \ldots, u_m)$ belongs to an open set $U \subset \mathbf{R}^m$. The problem is the following one: *Given any two points x_0 and $x_1 \in \Omega$, among all the piecewise continuous controls $u(t)$ transferring the point from x_0 to x_1 find the one which minimizes the functional $J = \int_{t_0}^{t_1} f^0(x(t), u(t))dt$.*

Now, let us assume that are given a piecewise-smooth set N of dimension lower or equal to $n-1$, and $n+1$ piecewise-smooth sets $P^0, P^1, \ldots, P^n$ verifying

$$P^0 \subset P^1 \subset P^2 \subset \ldots \subset P^n = \Omega, \tag{13}$$

and a function v defined in Ω and taking its values in U. Now, we can introduce Boltianskii's definition of a regular synthesis.

Definition 9. *The sets, $N, P^0, \ldots, P^n$ and the function v effect a* regular synthesis *for (12) in the region Ω, if the following conditions are satisfied.*

- **A** *The set P^0 is the target point. Every smooth component of $P^i \setminus (P^{i-1} \cup N)$, $i = 1, \ldots, n$, is an i-dimensional smooth manifold in Ω; these components will be called* i-dimensional cells. *The function v is continuously differentiable on each cell and can be extended into a continuously differentiable function on the neighbourhood of the cell.*
- **B** *All the cells are grouped into cells of the* first *or* second *type (T_1 or T_2) in the following manner:*
  - **(1)** *If σ is a 1-dim cell of type T_1, then it is a segment of a phase trajectory solution of (12) approaching the target P^0 with a nonzero phase velocity. If σ is a i-dim cell of type T_1 $(i > 1)$, then through every point of σ, passes a unique trajectory solution of equation (12). Furthermore, there exists an $(i-1)$-dim cell $\Pi(\sigma)$ such that every trajectory solution of (12) leaves σ after a finite time, and strikes against the cell $\Pi(\sigma)$ at a nonzero angle and with a nonzero phase velocity.*

(2) *If σ is a $(i-1)$-dim cell of type T_2 $(i \geq 1)$, then, from any point of σ there issues a unique trajectory of (12), moving in an $(i+1)$-dim cell $\Sigma(\sigma)$ of type T_1. Moreover, the function $v(x)$ is continuously differentiable on $\sigma \cup \Sigma(\sigma)$.*

(3) *All 3-dim cells are of type T_1.*

C *The conditions $B(1)$, $B(2)$ and $B(3)$ ensure the possibility of extending the trajectories solutions of (12) from cell to cell.*[2] *It is required that each trajectory "pierces" cells of the second kind only a finite number of times. In this connection every trajectory terminates at the point O. We will refer to these trajectories as being* marked.

D *From every point of the set $\Omega \setminus N$ there exists a unique marked trajectory that leads to O. From every point of N there issues a trajectory, solution of (12), not necessarily unique and which is also said to be* marked.

E *All the marked trajectories are extremals.*

F *The value of the functional J computed along the marked trajectories ending at the point O, is a continuous function of the initial point. In particular, if several trajectories start from a point x_0 of N, then, J takes the same value in each case.*

From this definition, we can now express Boltianskii's sufficient optimality condition:

Theorem 6. If a regular synthesis is effected in the set Ω under the assumption that the derivatives $\frac{\partial f^i}{\partial x^j}$ and $\frac{\partial f^i}{\partial u^k}$ exist and are continuous, and that $f^0(x,u) > 0$, then all the marked trajectories are optimal (in the region Ω).

4 Shortest paths for the Reeds-Shepp car

4.1 The pioneer works by Dubins and Reeds and Shepp

The initial work by Dubins from 1957 considered a particle moving at a constant velocity in the plane, with a constraint on the average curvature of trajectories. Using techniques close to those involved in the proof of Fillipov's existence theorem, Dubins proved the existence of shortest paths for his problem. He showed that the optimal trajectories are necessarily made up with arc of circles C of minimal turning radius and line segments S. Therefore, he proved that any optimal path must be of one of the following two path types:

$$\{C_a C_b C_e \, , C_a S_d C_e\} \quad \text{where: } 0 \leq a, e < 2\pi, \ \pi < b < 2\pi, \ \text{ and } \ d \geq 0 \qquad (14)$$

[2] Trajectories are extended from the cell σ into $\Pi(\sigma)$ if $\Pi(\sigma)$ is of type T_1, and from σ to $\Sigma(\Pi(\sigma))$ if $\Pi(\sigma)$ is of type T_2.

In order to specify the direction of rotation the letter C will sometimes be replaced by a "r" (right turn) or a "l" (left turn). The subscripts a, e, ... specify the length of each elementary piece.

Later, Reeds and Shepp [31] considered the same problem, when backwards motions are allowed ($|u_1| = k$). In both cases, as the modulus of the linear velocity keeps constant, the shortest path problem is equivalent to the minimum-time problem. Contrary to Dubins, Reeds and Shepp did not prove the existence of optimal paths. Indeed, as the control set is no more convex the existence of optimal paths cannot be deduced directly from Fillipov's theorem. From Dubins's result, they deduced that any subpath of an optimal path, lying between two consecutive cusp-points, must belong to the sufficient family (14). Finally, they proved that the search for a shortest path may be restricted to the following sufficient family (the symbol | indicates a cusp):

$$\begin{array}{l}\{\ C|C|C,\ \ CC|C,\ \ C|CC,\ \ CC_a|C_aC,\ \ C|C_aC_a|C,\\ C|C_{\pi/2}SC,\ \ CSC_{\pi/2}|C,\ \ C|C_{\pi/2}SC_{\pi/2}|C,\ \ CSC\ \}\end{array} \tag{15}$$

However the techniques used by Reeds and Shepp in their proof are based on specific *ad hoc* arguments from differential calculus and geometry, specially developed for this study, and cannot constitute a framework for further studies.

The following two subsections present a sequence of more recent works based on optimal control theory and geometry which have led to characterize the complete solution of Reeds and Shepp's problem. Section (4.2) presents a result simultaneously obtained by Sussmann and Tang [36] on the one hand, and by Boissonnat, Cerezo and Leblond [2] on the other hand, showing how Reeds and Shepp's result can be found and even slightly improved by using optimal control theory.

Section (4.3) presents a work by Souères and Laumond [33] who achieved the characterization of shortest paths by completing the local reasoning of PMP with global geometric arguments.

The last section (section 4.4) concludes the study by providing, a posteriori, a new proof of the construction by using Boltianskii's sufficient conditions [35].

4.2 Characterization of a sufficient family: A local approach

This section summarizes the work by Sussmann and Tang [36]; we use the notations introduced by the authors.

The structure of commutations As the control set $U_{RS} = \{-1, +1\} \times [-1, 1]$ related to Reeds and Shepp's problem (RS) is not convex, it is not

possible to deduce the existence of optimal paths directly from Fillipov's existence theorem. For this reason, the authors have chosen to consider what they call the *convexified problem* (CRS) corresponding to the convexified control set $U_{CRS} = [-1, +1] \times [-1, +1]$ for which Fillipov's existence theorem (theorem 2) applies. The existence of optimal paths for RS will be established *a posteriori* as a byproduct.

Let $g_1(x) = \begin{pmatrix} \cos\theta \\ \sin\theta \\ 0 \end{pmatrix}$, and $g_2(x) = \begin{pmatrix} 0 \\ 0 \\ 1 \end{pmatrix}$ denote the two vector fields on which the kinematics of the point is defined. With this notation system (2) becomes :

$$\dot{x} = f(x, u) = g_1(x)\ u_1 + g_2(x)\ u_2 \tag{16}$$

the corresponding hamiltonian is:

$$H = < \psi, f > = \ \psi_1 \cos\theta\ u_1 + \psi_2 \sin\theta\ u_1 + \psi_3\ u_2 = \phi_1\ u_1 + \phi_2\ u_2$$

where $\phi_1 = < \psi, g_1 >$, and $\phi_2 = < \psi, g_2 >$ represent the switching functions. From PMP, a necessary condition for $(u_1(t), u_2(t))$ to be an optimal control law, is that there exists a constant $\psi_0 \leq 0$ such that at each time $t \in [t_0, t_1]$

$$\begin{aligned} -\psi_0 &= < \psi(t), g_1(x(t)) > u_1(t) + < \psi(t), g_2(x(t)) > u_2(t) \\ &= \max_{v=(v_1,v_2)\in U}(< \psi(t), g_1(x(t)) > v_1(t) + < \psi(t), g_2(x(t)) > v_2(t)) \end{aligned} \tag{17}$$

$$\text{and } \ \dot{\psi}(t) = \frac{-\partial H}{\partial x}(\psi(t), x(t), u(t)) = -\psi(t)\ [u_1 \frac{dg_1}{dx} + u_2 \frac{dg_2}{dx}]$$

A necessary condition for t to be a switching time for u_i is that $\phi_i = 0$. Therefore, on any subinterval of $[t_0, t_1]$ where the switching function ϕ_i does not vanish the corresponding control component u_i is *bang* i.e. maximal or minimal.

Now, by means of theorem 4 we can express the derivative of the switching functions in terms of Lie brackets:

$$\begin{aligned} \phi_1 =< \psi, g_1 > &\Longrightarrow\ \dot{\phi}_1 = u_2 < \psi, [g_2, g_1] > \\ \phi_2 =< \psi, g_2 > &\Longrightarrow\ \dot{\phi}_2 = -u_1 < \psi, [g_2, g_1] > \end{aligned}$$

Thus the function $\phi_3 =< \psi, g_3 >$, where $g_3 = [g_1, g_2] = (-\sin\theta, \cos\theta, 0)^T$, seems to play an important role in the search for switching times. We have then:

$$\dot{\phi}_1 = u_2\phi_3 \ , \ \dot{\phi}_2 = -u_1\phi_3 \ , \ \dot{\phi}_3 = -u_2\phi_1 \tag{18}$$

Maximizing the Hamiltonian leads to:

$$u_1(t) = \text{sign}(\phi_1(t)) \quad \text{and} \quad u_2(t) = \text{sign}(\phi_2(t)) \tag{19}$$

$$\text{where} \quad \text{sign}(s) = \begin{cases} +1 & \text{if } s > 0 \\ -1 & \text{if } s < 0 \\ \text{any element of [-1,1]} & \text{if } s = 0 \end{cases}$$

Then from PMP we get:

$$|\phi_1(t)| + |\phi_2(t)| + \psi_0 = 0 \tag{20}$$

On the other hand, at each point of the manifold M, the vector fields g_1, g_2 and g_3 define a basis of the tangent space. Therefore, as the adjoint vector never vanishes, ϕ_1, ϕ_2 and ϕ_3 cannot have a common zero. It follows that:

$$|\phi_1(t)| + |\phi_2(t)| + |\phi_3(t)| \neq 0 \tag{21}$$

Equations (18), (19), (20) and (21) define the structure of commutations; several properties may be deduced from these relations as follows:

Lemma 1. There do not exist (non trivial) abnormal extremals for CRS.

Proof: If $\psi_0 = 0$ then (20)$\Longrightarrow \phi_1 \equiv 0$ and $\phi_2 \equiv 0$. Then (21)$\Longrightarrow \phi_3 \neq 0$ but (18) $\Longrightarrow u_1\phi_3 = u_2\phi_3 = 0 \Longrightarrow u_1 = u_2 = 0$. The only remaining possibility is a trivial trajectory i.e. of zero length in zero time □.

Lemma 2. On a non trivial extremal trajectory for CRS, ϕ_1 and ϕ_2 cannot have a common zero.

Proof: If $\exists t \in [t_0, t_1]$ such that $\phi_1(t) = \phi_2(t) = 0$ then (20) $\Longrightarrow \psi_0 = 0$, we conclude with lemma 1 □

Lemma 3. Along an extremal for CRS $\kappa = \phi_1^2 + \phi_3^2$ is constant. Furthermore, $(\kappa = 0) \Longleftrightarrow (\phi_1 \equiv 0)$

Proof: As $\dot{\phi}_1 = u_2\phi_3$ and $\dot{\phi}_3 = u_2\phi_1$ we deduce that $\kappa = \phi_1^2 + \phi_3^2$ is constant. $\kappa = 0 \Rightarrow \phi_1 \equiv 0$, obvious. Inversely, suppose $\phi_1 \equiv 0$ but $\kappa \neq 0$; from lemma 2 it follows that $\phi_2 \neq 0$. Therefore as $u_2 = sign(\phi_2)$, $u_2 \neq 0$. But then (18) $\Longrightarrow 0 = \dot{\phi}_1 = u_2.\phi_3 \Longrightarrow \phi_3 = 0$ that leads to a contradiction □.

Lemma 4. Along an extremal for CRS, either the zeros of ϕ_1 are all isolated, or $\phi_1 \equiv 0$. Furthermore, at an isolated zero of ϕ_1, $\dot{\phi}_1$ exists and does not vanish.

Proof: Let $x(t,u)$ be an extremal for CRS on $[t_0,t_1]$. Suppose $\phi_1 \not\equiv 0$; it follows that $\kappa > 0$. Let $\tau \in]t_0,t_1[$ such that $\phi_1(\tau) = 0$, from lemma 2 $\phi_2(\tau) \neq 0$ and as ϕ_2 is continuous there exists a subinterval $I \subset]t_0,t_1[$ containing τ such that $\forall t \in I, \phi_2(t) \neq 0$. Therefore the sign of ϕ_2 is constant on I. From this, we deduce that $u_2 \equiv 1$ or $u_2 \equiv -1$ on I. In either case, since the equation $\dot{\phi}_1 = u_2(t)\ \phi_3(t)$ holds on I, it comes $\dot{\phi}_1(t) = \pm\phi_3(t)$, the sign keeping constant on I. $\kappa > 0$ and $\phi_1(\tau) = 0 \implies \phi_3(\tau) \neq 0 \implies \dot{\phi}_1(\tau) = \pm\phi_3(\tau) \neq 0$. therefore, τ is an isolated zero. □

Therefore, there exist two kinds of extremal trajectories for CRS:

- type A: trajectories with a finite number of switch on u_1,
- type B: trajectories along which $\phi_1 \equiv 0$ and either $u_2 \equiv 1$ or $u_2 \equiv -1$.

Before starting the study of these two path types, we need to state a simple preliminary lemma.

Lemma 5. If an optimal trajectory for CRS is an arc bang C_a then necessarily $a \leq \pi$.

Proof: When $a > \pi$ it suffice to follow the arc of length $2\pi - a$ in the opposite direction. □

Characterization of type A trajectories First, let us consider the type A trajectories with **no cusp** i.e. trajectories along which $u_1 \equiv 1$ or $u_1 \equiv -1$. According to the symmetry of the problem we can restrict the study to the case that $u_1 \equiv 1$. The corresponding trajectories are the solutions of Dubins' problem (DU) which are optimal for CRS.

Let $\gamma(t), t \in [t_0,t_1]$ be such a trajectory. From lemma 4 we know that the zeros of ϕ_1 are all isolated. Furthermore, ϕ_1 cannot vanish on $]t_0,t_1[$ because in that case the sign of ϕ_1 would have to change, and u_1 would have to switch. Therefore, as γ is a trajectory for DU, $\phi_1(t) \geq 0$ on $[t_0,t_1]$ and $\phi_1 > 0$ on $]t_0,t_1[$. Equations (18) become: $\dot{\phi}_2 = -\phi_3$ and $\dot{\phi}_3 = -u_2\phi_1$. Then ϕ_2 is of class $\mathcal{C}^1$ and $\ddot{\phi}_2 = u_2\phi_1$. Furthermore, $u_2 = \text{ sign}(\phi_2)$, then $\ddot{\phi}_2 = \phi_1 \text{sign}(\phi_2)$. This means that ϕ_2 is convex, (resp. concave) on the whole interval where $\phi_2 > 0$ (resp. $\phi_2 < 0$). From that we deduce the following property:

Lemma 6. A trajectory γ with no cusp, optimal for CRS, is necessarily of one of the following three kinds:

- $C_a \quad 0 \leq a \leq \pi$

- $C_a C_b \quad 0 < a \leq \frac{\pi}{2} \quad \text{and} \quad 0 < b \leq \frac{\pi}{2}$
- $C_a S_c C_b \quad 0 < c\,, \quad 0 \leq a \leq \frac{\pi}{2} \quad \text{and} \quad 0 \leq b \leq \frac{\pi}{2}$

Proof:

As before we consider only the trajectories along which $u_1 \equiv 1$. If ϕ_2 does not vanish, γ is an arc bang; from lemma 5 we can conclude.

If ϕ_2 vanishes, let us denote by I the time interval defined by $I = \{t, t \in [t_0, t_1], \phi_2(t) \neq 0\}$. As $\phi_2^{-1}(0)$ is closed, I is relatively open in $[t_0, t_1]$. Let $\mathcal{I}$ be the set of connected components of I. First, let us prove that $\mathcal{I}$ does not contain any open interval $J =]t', t''[\subset [t_0, t_1]$. Indeed, if J is such an interval, then $\phi_2(t') = \phi_2(t'') = 0$. Since ϕ_2 is either negative and concave, or positive and convex on J, then necessarily $\phi_2 \equiv 0$ on J which is a contradiction. So $[t_0, t_1]$ is partitioned into at most three intervals I_1, I_2, I_3 such that ϕ_2 never vanishes on $I_1 \cup I_3$, and $\phi_2 \equiv 0$ on I_2. On each interval J in $\mathcal{I}$ u_2 is constant and equals 1 or -1. From equations (18) we get $\ddot{\phi}_3 + \phi_3 = 0$. We have shown that ϕ_2 vanishes on $I_2 = [t', t'']$; if $t_0 < t'$ then ϕ_2 is convex and positive (or concave and negative) on $[t_0, t'[$ and $\phi_2(t') = 0$. Therefore both ϕ_3 and $\dot{\phi}_3$ have a constant sign on $]t_0, t'[$ (for instance, if $\phi_2 > 0$ on $[t_0, t'[$, then $\dot{\phi}_3 = -u_2\phi_1$ and $u_2 = -sign(\phi_2) = -1 \Rightarrow \dot{\phi}_3 = \phi_1 \neq 0$). Also $\phi_3 = -\dot{\phi}_2$, so ϕ_3 has no zero either because the derivative of a convex function only vanishes at its minimum. This implies that $t' - t_0 \leq \frac{\pi}{2}$. By applying a same reasoning on $]t'', t_1]$ we conclude the proof for the case $u_1 \equiv 1$. The case $u_1 \equiv -1$ can be derived from the same arguments □.

Remark 5. *The previous lemma does not solve Dubins' problem. It just determines the structure of Dubins' trajectories which are CRS-optimal. Indeed, a time optimal trajectory for DU is not necessarily optimal for CRS.*

Now let us go back to the general form of type A trajectories. By integrating the adjoint equations type A trajectories may be very well characterized. Let us consider the adjoint system:

$$\begin{cases} \dot{\psi}_1 = -\frac{\partial H}{\partial x} = 0 \\ \dot{\psi}_2 = -\frac{\partial H}{\partial y} = 0 \\ \dot{\psi}_3 = -\frac{\partial H}{\partial \theta} = \psi_1 \sin\theta\, u_1 - \psi_2 \cos\theta\, u_1 = \psi_1\, \dot{y} - \psi_2\, \dot{x} \end{cases}$$

Hopefully, these equations are easily integrable: ψ_1 and ψ_2 are constant on $[t_0, t_1]$ and if we suppose $x(t_0) = y(t_0) = 0$ we get $\phi_2(t) = \psi_3(t) = \psi_3(t_0) + \psi_1 y(t) - \psi_2 x(t)$. Therefore, from relation (17) we can deduce that the switching points are located on three parallel lines.

- when $\phi_2(t) = 0$, the point lies on the line D_0: $\psi_1 y - \psi_2 x + \psi_3(t_0) = 0$
- when $\phi_1(t) = 0$, we deduce from (17) that $\psi_3(t)u_2(t) + \psi_0 = 0$:
  - If $u_2 = 1$ the point is on the line $D^+ : \psi_1 y - \psi_2 x + \psi_3(t_0) + \psi_0 = 0$
  - If $u_2 = -1$ the point is on the line $D^- : \psi_1 y - \psi_2 x + \psi_3(t_0) - \psi_0 = 0$

- If $\phi_2(t)$ vanishes over a non empty interval $[\tau_1, \tau_2] \subset [t_0, t_1]$, we get from relation (17): $\psi_1 \cos\theta(t) + \psi_2 \sin\theta(t) + \psi_0 = 0$. According to lemma 2, the constant ψ_1 and ψ_2 cannot be both zero, it follows that θ remains necessarily constant on $[\tau_1, \tau_2]$, the singular control component u_2 is equal to 0, and the corresponding trajectory is a segment of D_0.

- At a cusp point $\phi_1 = \psi_1 \cos\theta + \psi_2 \sin\theta = 0$. It follows that the point is oriented perpendicularly to the common direction of the three lines.

To sum up, type A trajectories are made up with arcs of circle (C) of minimal turning radius which correspond to the regular control laws $(u_1 = \pm 1, u_2 = \pm 1)$ and line segments (S) which correspond to the singularity of the second control component: $(u_1 = \pm 1, u_2 = 0)$. The line segments and the point of inflection are on D_0, the cusp point are on D^+ or D^- and at each cusp the direction of the point is perpendicular to the common direction of the lines, see figure (3). We have the following lemma:

Lemma 7. In the plane of the car's motion any trajectory of type A is located between two parallel lines D^+ and D^-. The points of inflection and the line segments belong to a third line D_0 having the same direction as D^+ and D^- and located between them at equal distance $|\frac{\psi_0}{\psi_1}| \leq \frac{\pi}{2}$. The cusp-points are located on D^+ when $u_2 = 1$ and on D^- when $u_2 = -1$; at a cusp point the representative point's orientation is perpendicular to these lines.

At this stage, by using a geometric reasoning it is possible to prove that some sequences of arcs and line segments are never optimal.

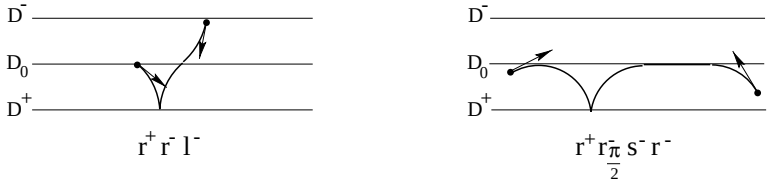

Fig. 3. Optimal paths of type (**A**) lie between two parallel lines D^+ and D^-.

Lemma 8. The following trajectories cannot be CRS-optimal paths.

1. $C_a|C_\pi \qquad a > 0$
2. $C_a|C_{\frac{\pi}{2}} S_e C_{\frac{\pi}{2}} \quad a > 0, e \geq 0$, with the same direction of rotation (l or r) on the arcs $C_{\frac{\pi}{2}}$ located at each extremity of S.
3. $C_{\frac{\pi}{2}} S_e C_{\frac{\pi}{2}} | C_{\frac{\pi}{2}}$, $e \geq 0$, with an opposite direction of rotation on the arcs $C_{\frac{\pi}{2}}$ located at each extremity of S.

4. $C_a|C_bC_b|C_bC_b \quad a, b > 0$

Proof: The method of the proof consists in showing that each trajectory is equivalent to another one which is clearly not optimal. The reasoning is illustrated at figure (4): By replacing a part of the initial path by the equivalent one drawn in dotted line, we get an equivalent trajectory i.e. having the same cost and linking the same two configurations. Then, using the preceding lemmas 6 and 7 we prove that this new trajectory does not verify the necessary conditions of PMP. On figure (4) the path 1, $l_a^+ l_\pi^-$ is equivalent to a path $l_a^+ r_\pi^+$ and from lemma 6 we now that such a path is not optimal. The three other path types (2, 3 and 4) do not satisfy lemma 7. Indeed, either the points of inflection and the line segment do not belong to the same line D_0 or the direction of the point at a cusp is not perpendicular to D_0. □

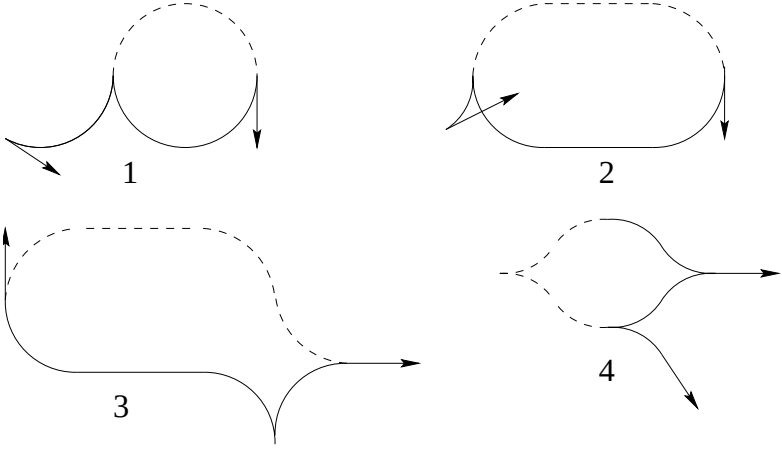

Fig. 4. Non-optimal equivalent trajectories

Finally, Using the theory of envelopes, Sussmann and Tang showed that a path $C_a|C_bC_b|C_b$ is never optimal. Due to the lack of space we cannot present here this technical part of the proof, the reader will have to refer to [36]. This last result eliminates type A trajectories with more than two cusps. The remaining possible sequences of (C) and (S) determine eight path types which are represented by the types (II) to (IX) of the sufficient family (22) presented at section 4.2.

Characterization of type B trajectories Let us first consider the case that $u_2 \equiv 1$; we call this subproblem LTV (Left Turn Velocity). In order to lead their

reasoning the authors considered what they called the lifted problem LLTV (Lifted Left Turn Velocity) obtained from LTV by regarding the variable θ as a real number x_3. For this last problem, as $\dot{x_3} \equiv 1$, any trajectory γ linking the point x_0 at time t_0 to the point x_1 at time t_1 has the cost: $\Delta t = x_3(t_1) - x_3(t_0)$. The same phenomenon occurs for LTV, but only for trajectories whose duration is lower or equal to π. For this reason the problem LLTV is called degenerate whereas the problem LTV is locally degenerate.

Using the techniques presented in chapter 1 it is straight forward to deduce from the structure of the Lie algebra $L = Lie(g_1, g_2)$ generated by the vector fields g_1 and g_2, that the problem LTV has the accessibility property. Nevertheless, as the corresponding system is not symmetric (i.e. an admissible trajectory followed backwards is not necessary admissible) we cannot deduce directly the controllability of LTV. This can be done by considering the "bang-bang" system (BB) corresponding to the control set $(u_1, u_2) \in \{-1, +1\} \times \{-1, +1\}$. As the BB system has the accessibility property and is symmetric on the connected manifold $\mathbf{R}^2 \times S^1$ it is controllable. Any admissible trajectory for BB is a sequences of tangent arcs C. By replacing every arc r_α by the complementary part $l_{2\pi-\alpha}$ followed backwards, we can transform any BB trajectory into an admissible trajectory for LTV. Therefore, we deduce the controllability of the problem LTV. This is no more true for the problem LLTV in $\mathbf{R}^3$. It suffice to note that no point $(x, y, 0)$ verifying $(x, y) \neq (0, 0)$ is reachable from the origin.

By using the Ascoli-Arzelà theorem, Sussmann and Tang proved that the reachable set for LLTV from x_0, $\mathcal{R}(x_0)$, is a closed subset of $\mathbf{R}^3$. Now, let L_0 be the ideal of the lie algebra L generated by g_1. As L_0 is the smallest linear subspace S of L, such that $\forall X \in S, \forall Y \in L, [X, Y] \in S$. It follows that $L_0 = Lie(g_1, g_3)$.

Definition 10. *(Sussmann) - L_0 is called* strong accessibility Lie algebra.

- Let $x \in \mathbf{R}^3$, $L_0(x) = span(g_1(x), g_2(x))$; a trajectory of LLTV is called a strong extremal *if the corresponding adjoint vector ψ is not trivial on $L_0(\gamma(t))$, i.e. the projection of $\psi(t)$ on $L_0(\gamma(t))$ never vanishes.*

- We will call boundary trajectory *of LLTV any trajectory $\gamma : [t_0, t_1] \to \mathbf{R}^3$ such that $\gamma(t_1)$ belongs to the boundary $\partial\mathcal{R}(x_0)$ of $\mathcal{R}(x_0)$.*

Lemma 9. Any boundary trajectory of LLTV is a strong extremal of the form $l_a^{s_0} l_\pi^{s_1} \dots l_\pi^{s_k} l_b^{s_{k+1}}$ where $0 \leq a, b \leq \pi$ and the signs $s_i \in \{+, -\}$ alternate.

Proof: Let $\gamma : [t_0, t_1] \to \mathbf{R}^3$ be a boundary trajectory for LLTV, $x_0 = \gamma(t_0)$ and $x_1 = \gamma(t_1) \in \partial\mathcal{R}(x_0)$. From theorem 5 we know that there exists a nontrivial adjoint vector $\psi = (\psi_0, \psi_1, \dots, \psi_n)$ verifying $\psi_0 \equiv 0$. From relation (20) we get $|\phi_1| + |\phi_2| = 0$. On the other hand, $\kappa = \phi_1(t)^2 + \phi_3(t)^2 \neq 0$ otherwise $\phi_1 = \phi_2 = \phi_3 = 0$. It follows that $< \psi, g_1 >= \phi_1$ and $< \psi, g_2 >= \phi_3$ do not vanish simultaneously and therefore γ is a strong extremal for LLTV. Now, as $u_2 \equiv 1$ we know from equations (18) that

ϕ_1 must be a nontrivial solution of $\ddot{\phi_1} + \phi_1 = 0$. Therefore, the distance between two consecutive zeros of ϕ_1 is exactly π and the sign of ϕ_1 changes at each switch. □

Lemma 10. Given any path γ solution of LLTV, there exists an equivalent solution γ' of LLTV which is a concatenation of a boundary trajectory and an arc bang of LLTV for the control $u_1 \equiv 1$.

Proof: Let γ be defined on $[t_0, t_1]$, $\gamma(t_0) = x_0$ and $\gamma(t_1) = x_1$ a trajectory solution of LLTV. If $x_1 \in \partial\mathcal{R}(x_0)$ the conclusion follows. Suppose now that $x_1 \in Int(\mathcal{R}(x_0))$. let us consider an arc bang for LLTV corresponding to the control $u_1 \equiv 1$, ending at x_1. As the set $\mathcal{R}(x_0)$ is closed, by following this path backwards from x_1 the representative point reaches, after a finite time, a point x_1' belonging to the boundary. The problem being degenerate, the trajectory γ made up by the boundary trajectory from x_0 to x_1' followed by the arc bang from x_1' to x_1 is equivalent to γ. □

Now Suppose $\gamma : [t_0, t_1] \to \mathbf{R}^2 \times S^1$ is an LTV trajectory time optimal for CRS. Let $\pi : \mathbf{R}^3 \to \mathbf{R}^2 \times S^1$ be the canonical projection, then $\gamma = \pi \circ \gamma^\star$ where $\gamma^\star : [t_0, t_1] \to \mathbf{R}^3$ is a trajectory of LLTV. From the previous lemma we can replace $\gamma^\star$ by the concatenation $\gamma^\star_{new}$ of a boundary trajectory $\gamma_1^\star$ and a bang trajectory $\gamma_2^\star$ for $u_1 \equiv 1$, and then project these down to trajectories γ_{new}, γ_1, γ_2 in $\mathbf{R}^2 \times S^1$. Then γ_1 is of the form $l_a^{s_0} l_\pi^{s_1} \dots l_\pi^{s_k} l_b^{s_{k+1}}$. But from lemma 8 a path $C_a|C_\pi$ with $a > 0$ cannot be optimal. It follows that γ_1 contains at most one cusp, and the length of γ_2 is lower or equal to π. Therefore, γ_{new} is a path $l_a^+ l_b^- l_c^+$ or $l_a^- l_d^+ l_e^+ = l_a^- l_{d+e}^+$ with a, b, c and $d + e$ at most equal to π. Hence, the type $l_a^+ l_b^- l_c^+, 0 \le a, b, c \le \pi$ constitutes a sufficient family for LLTV.

Using the same reasoning for the dual problem RTV (Right Turn Velocity), the path type $r_a^+ r_b^- r_c^+$ with $0 \le a, b, c \le \pi$ appears to be also sufficient.

Remark 6. *The reasoning above cannot be directly held in* $\mathbf{R}^2 \times S^1$ *for LTV because in this case the length of a trajectory steering the point from* x_0 *to* x_1 *is not necessarily equal to* $\theta(t_1) - \theta(t_0)$.

Sufficient family for RS From the reasoning above it appears that the search for optimal trajectories for CRS may be restricted to the following sufficient family containing nine path types:

(I)	$l_a^+ l_b^- l_e^+$ or $r_a^+ r_b^- r_e^+$	$0 \le a \le \pi\ ,\ 0 \le b \le \pi\ ,\ 0 \le e \le \pi$
$(II)(III)$	$C_a\|C_b C_e$ or $C_a C_b\|C_e$	$0 \le a \le b\ ,\ 0 \le e \le b\ ,\ 0 \le b \le \frac{\pi}{2}$
(IV)	$C_a C_b\|C_b C_e$	$0 \le a < b\ ,\ 0 \le e < b\ ,\ 0 \le b \le \frac{\pi}{2}$
(V)	$C_a\|C_b C_b\|C_e$	$0 \le a < b\ ,\ 0 \le e < b\ ,\ 0 \le b \le \frac{\pi}{2}$
(VI)	$C_a\|C_{\frac{\pi}{2}} S_l C_{\frac{\pi}{2}}\|C_b$	$0 \le a < \frac{\pi}{2}\ ,\ 0 \le b < \frac{\pi}{2}\ ,\ 0 \le l$
$(VII)(VIII)$	$C_a\|C_{\frac{\pi}{2}} S_l C_b$ or $C_b S_l C_{\frac{\pi}{2}}\|C_a$	$0 \le a \le \pi\ ,\ 0 \le b \le \frac{\pi}{2}\ ,\ 0 \le l$
(IX)	$C_a S_l C_b$	$0 \le a \le \frac{\pi}{2}\ ,\ 0 \le l\ ,\ 0 \le b \le \frac{\pi}{2}$

(22)

However, all the path contained in this family are obtained for $u_1 = 1$ or $u_1 = -1$, and by this, are admissible for RS. Therefore, this family constitutes also a sufficient family for RS which contains 46 path types. This result improves slightly the preceding statement by Reeds and Shepp of a sufficient family containing 48 path types.

On the other hand, as Fillipov's existence theorem guarantees the existence of optimal trajectories for the convexified problem CRS, it ensures the existence of shortest paths with bounded curvature radius for linking any two configurations of Reeds and Shepp's car. Applying PMP to Reeds and Shepp's problem we deduce the following lemma that will be useful in the sequel.

Lemma 11. (Necessary conditions of PMP)
Optimal trajectories for RS are of two types:

- **A/** Paths lying between two parallel lines D^+ and D^- such that the straight line segments and the points of inflection lie on the median line D_0 of both lines, and the cusp points lie on D^+ or D^-. At a cusp the point's orientation is perpendicular to the common direction of the lines (see figure 3),
- **B/** Paths $C|C|\ldots|C$ with $length(C) \leq \pi$ for any C.

4.3 A geometric approach: construction of a synthesis of optimal paths

Symmetry and reduction properties In order to analyse the variation of the car's orientation along the trajectories let us consider the variable θ as a real number. To a point $q = (x, y, \theta^*)$ in $\mathbf{R}^2 \times S^1$ correspond a set $Q = \{(x, y, \theta) \ / \ \theta \in \theta^*\}$ in $\mathbf{R}^3$ where θ^* is the class of congruence modulus 2π. Therefore, the search for a shortest path from q to the origin in $\mathbf{R}^2 \times S^1$ is equivalent to the search for a shortest path from Q to the origin in $\mathbf{R}^3$. By considering the problem in $\mathbf{R}^3$ instead of $\mathbf{R}^2 \times S^1$ we can point out some interesting symmetry properties. First let us consider trajectories starting from each horizontal plane $P_\theta = \{(x, y, \theta),\ x, y \in \mathbf{R}^2\} \subset \mathbf{R}^3$.

In the plane P of the robot's motion, or in the plane P_θ, we denote by Δ_θ the line of equation: $y = -x \cot \frac{\theta}{2}$ and $\Delta_\theta^\perp$ the line perpendicular to Δ_θ passing through 0. Given a point (M, θ), we denote by M_1 the point symmetric to M with respect to O, M_2 the point symmetric to M with respect to Δ_θ, and M_3 the point symmetric of M_1 with respect to Δ_θ. Let $\mathcal{T}$ a be path from (M, θ) to $(O, 0)$.

Lemma 12. There exist three paths $\mathcal{T}_1$, $\mathcal{T}_2$ and $\mathcal{T}_3$ each isometric to $\mathcal{T}$, starting respectively from (M_1, θ), (M_2, θ) and (M_3, θ) and ending at $(O, 0)$ (see figure 5).

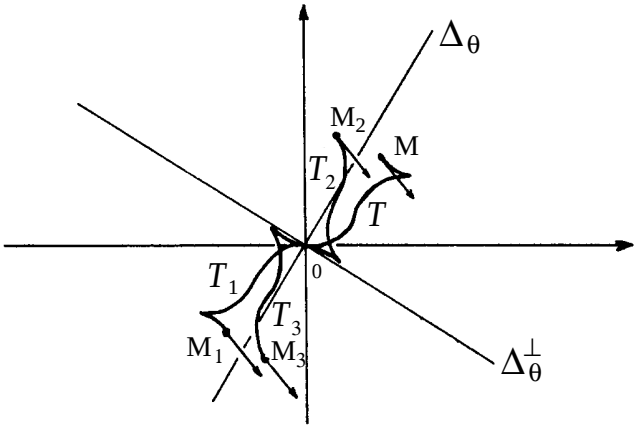

Fig. 5. A path gives rise to 3 isometric ones.

Proof: (see Figure 5) $\mathcal{T}_1$ is obtained from $\mathcal{T}$ by the symmetry with respect to O.

Proving the existence of $\mathcal{T}_2$ requires us to consider the construction illustrated at figure (6): We denote by δ the line passing through M and making an angle θ with the x-axis, and s the axial symmetry with respect to δ. Let A be the intersecting point of δ with the x-axis and r the rotation by the angle $-\theta$ around A. Let us note $L = r(M)$. Finally, t, represents the translation of vector $\overrightarrow{LO}$. We denote by $\mathcal{T}_2$ the image of $\mathcal{T}$ by the isometry $\Im = t \circ r \circ s$. $\mathcal{T}_2$ links the directed point $(\tilde{M}, \tilde{\theta}) = \Im((O, 0))$ to $(O, 0) = \Im(M, \theta)$. $\tilde{\theta}$ clearly equals θ. We have to prove that $\tilde{M} = M_2$. Let respectively α and β be the angles made by (O, M) and $(O, \tilde{M})$ with the x-axis. The measure of the angle made by the bisector of $(\widehat{M, O, \tilde{M}})$ and the x-axis is: $\alpha + \frac{\beta - \alpha}{2} = \frac{\alpha + \beta}{2} = \frac{\pi - \theta}{2}$. As $\tan \frac{\pi - \theta}{2} = -\cot \frac{\theta}{2}$, we can assert that $\tilde{M}$ is the symmetric point of M with respect to Δ_θ, i.e. M_2.

Finally $\mathcal{T}_3$ is obtained as the image of $\mathcal{T}$ by $\Im$ followed by the symmetry with respect to the origin. □

Lemma 13. If $\mathcal{T}$ is a path from $(M(x, y), \theta)$ to $(O, 0)$, there exists a path $\overline{\mathcal{T}}$, isometric to $\mathcal{T}$, from $(\overline{M}(x, -y), -\theta)$ to $(O, 0)$.

Proof: It suffices to consider the symmetry s_x with respect to the abscissa axis.

Remark 7.
- *By combining the symmetry with respect to Δ_θ and the symmetry with respect to O, the line $\Delta_\theta^\perp$ appears to be also an axis of symmetry. According to lemmas 12 and 13 it is enough to consider paths starting from one quadrant in each plane P_θ, and only for positive or negative values of θ.*
- *The constructions above allow us to deduce easily the words w_1, w_2, w_3 and w_4 describing $\mathcal{T}_1$, $\mathcal{T}_2$, $\mathcal{T}_3$ and $\mathcal{T}_4$ from the word w describing $\mathcal{T}$.*

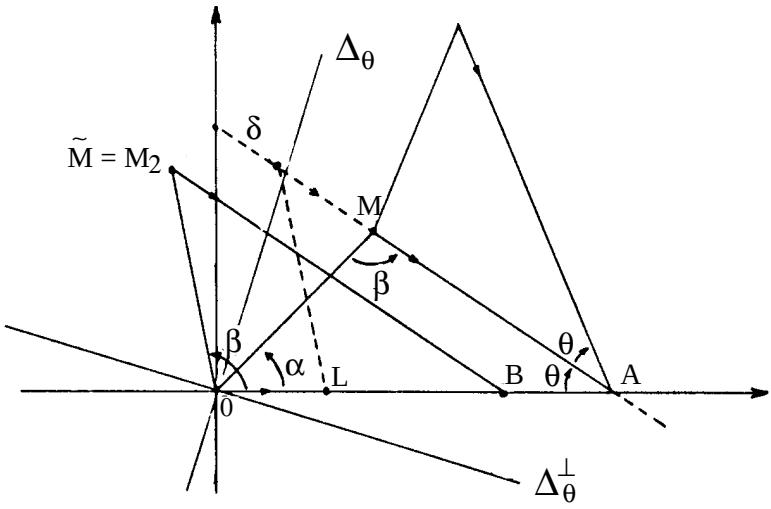

Fig. 6. Construction of the isometry $\Im$.

- *w_1 is obtained by writing w, then by permutating the superscripts $+$ and $-$*
- *w_2 is obtained by writing w in the reverse direction, then by permutating the superscripts $+$ and $-$*
- *w_3 is obtained by writing w in the reverse direction*
- *$\overline{w}$ is obtained by writing w, then by permutating the r and the l* □

As a consequence of both lemmas above a last symmetry property holds in the case that $\theta = \pm\pi$:

Lemma 14. If $\mathcal{T}$ is a path from $(M(x,y),\pi)$ (resp. $(M(x,y),-\pi)$) to $(O,0)$, there exists an isometric path $\mathcal{T}'$ from $(M(x,y),-\pi)$ (resp. $(M(x,y),\pi)$) to $(O,0)$.

The word w' describing $\mathcal{T}'$ is obtained by writing w in the opposite direction, then by permutating on the one hand the r and the l, and on the other hand the $+$ and $-$.

Remark 8. *The points $(M(x,y),\pi)$ and $(M(x,y),-\pi)$ represent the same configuration in $\mathbf{R}^2 \times S^1$ but are different in $\mathbf{R}^3$. This means that the trajectories $\mathcal{T}$ and $\mathcal{T}'$ are isometric and have the same initial and final points, but along these trajectories the car's orientation varies with opposite direction.*

Proof of lemma 14: We use the notation of lemma 12 and 13. Let $(M(x,y),\pi)$ be a directed point and $\mathcal{T}$ a trajectory from (M,π) to $(0,0)$. When $\theta = \pm\pi$ the axis

Δ_θ is aligned with the x-axis. By lemma 12, there exists a trajectory $\mathcal{T}_2 = \Im(\mathcal{T})$, isometric to $\mathcal{T}$, starting at $(M_2(x,-y),\pi)$ and ending at $(O,0)$. Then by lemma 12 there exists a trajectory $\overline{\mathcal{T}_2} = s_x(\mathcal{T}_2)$, isometric to $\mathcal{T}_2$, starting at $(\overline{M_2}(x,y),-\pi)$ and ending at $(O,0)$. Let us call $\mathcal{T}'$ the trajectory $\overline{\mathcal{T}_2}$, then $\mathcal{T}' = s_x \circ \Im(\mathcal{T})$ is isometric to $\mathcal{T}$ and by combining the rules defining the words w_2 and $\overline{w}$ we obtain the rule characterizing $\overline{w_2} = w'$ (the same reasoning holds when $\theta = -\pi$.) □

Now by using lemma 14 we are going to prove that it suffice to consider paths starting from points (x,y,θ) when $\theta \in [-\pi,\pi]$. In the family (22) three types of path may start with an initial orientation θ that does not belong to $[-\pi,\pi]$. These types are (I) and (VII) & (VIII). Combining lemma 14 with the necessary condition given by PMP we are going to refine the sufficient family (22) by rejecting those paths along which the total angular variation is greater than π.

Lemma 15. In the family (22), types *(I), (VII)* and *(VIII)* may be refined as follows:

(I) $\quad l_a^+ l_b^- l_e^+$ or $r_a^+ r_b^- r_e^+ \qquad 0 \le a+b+e \le \pi$

(VII)(VIII) $\quad C_a|C_{\frac{\pi}{2}} S_d C_b$ or $C_b S_d C_{\frac{\pi}{2}}|C_a$ $\begin{cases} 0 \le a \le \frac{\pi}{2}\ ,\ 0 \le b \le \frac{\pi}{2}\ ,\ 0 \le d \\ \text{and}\ \ a+b \le \frac{\pi}{2}\ \ \text{if}\ \ u_2\ \ \text{is constant} \\ \text{on every arc}\ C \end{cases}$

Proof: Our method is as follows:

1. We consider a path $\mathcal{T}$ linking a point (M,θ) to the origin, such that $|\theta| > \pi$.
2. We select a part of $\mathcal{T}$ located between two configurations (M_1,θ_1) and (M_2,θ_2) such that $|\theta_1 - \theta_2| = \pi$. According to lemma 14 we replace this part by an isometric one, along which the point's orientation rotates in the opposite direction. In this way we construct a trajectory equivalent to $\mathcal{T}$ i.e having the same length and linking (M,θ) to the origin.
3. We prove that this new trajectory does not verify the necessary conditions given by PMP. As $\mathcal{T}$ is equivalent to this non optimal path we deduce that it is not optimal.

Let us consider first a type (I) path. Due to the symmetry properties it suffices to regard a path $l_a^+ l_b^- l_e^+$ with $a+b+e = \pi+\epsilon, (\epsilon > 0)$ and $a > \epsilon$. If we keep in place a piece of length ϵ and replace the final part using lemma 14, we obtain an equivalent path $l_\epsilon^+ r_e^- r_b^+ r_{a-\epsilon}^-$ which is obviously not optimal because the robot goes twice to the same configuration.

We use the same reasoning to show that a path $C_a|C_{\frac{\pi}{2}} S_d$ with $d \neq 0$ cannot be optimal if $a > \frac{\pi}{2}$. Without lost of generality we consider a path $l_{\frac{\pi}{2}+\epsilon}^+ l_{\frac{\pi}{2}}^- s_d^-$. According to lemma 14 we can replace the initial piece $l_{\frac{\pi}{2}+\epsilon}^+ l_{\frac{\pi}{2}-\epsilon}^-$ by the isometric one $r_{\frac{\pi}{2}-\epsilon}^+ r_{\frac{\pi}{2}+\epsilon}^-$.

The initial path is then equivalent to the path $r^+_{\frac{\pi}{2}-\epsilon} r^-_{\frac{\pi}{2}+\epsilon} l^-_\epsilon s^-$ which cannot be optimal as the point of inflection do not belong to the line supporting the line segment.

Consider now a path $C_a|C_{\frac{\pi}{2}} S_d C_b$ or $C_b S_d C_{\frac{\pi}{2}}|C_a$ with u_2 constant on the arcs. We show that such a path cannot be optimal if $a+b > \frac{\pi}{2}$. Consider a path $l^+_a l^-_{\frac{\pi}{2}} s^-_d l^-_b$ with $a+b = \frac{\pi}{2}+\epsilon$ and $a > \epsilon$. We keep in place a piece of length ϵ and replace the final part by an isometric one according to lemma 14. We obtain an equivalent path $l^+_\epsilon r^+_b s^+_d l^+_{\frac{\pi}{2}} r^-_{a-\epsilon}$. As the point of inflection does not lie on the line D_0, this path violates both necessary conditions **A** and **B** of PMP (see lemma 11) and therefore is not optimal. □

Remark 9. *In the sufficient family (22) refined by lemma 15, the orientation of initial points is defined in* $[-\pi, \pi]$. *So, to solve the shortest path problem in* $\mathbf{R}^2 \times S^1$, *we only have to consider paths starting from* $\mathbf{R}^2 \times [-\pi, \pi]$ *in* $\mathbf{R}^3$.

Construction of domains For each type of path in the new sufficient family, we want to compute the domains of all possible starting points for paths ending at the origin. According to the symmetry properties it suffices to consider paths starting from one of the four quadrants made by Δ_θ and $\Delta^\perp_\theta$, in each plane P_θ, and only for positive or negative values of θ. We have chosen to construct domains covering the *first* quadrant (i.e. $x \tan\frac{\theta}{2} \leq y \leq -x \cot\frac{\theta}{2}$), for $\theta \in [-\pi, 0]$.

As any path in the sufficient family is described by three parameters, each domain is the image of the product of three real intervals by a continuous mapping. It follows that such domains are connected in the configuration space.

To represent the domains, we compute their restriction to planes P_θ. As θ is fixed, the cross section of the domain in P_θ is defined by two parameters. By fixing one of them as the other one varies, we compute a foliation of this set. This method allows us, on the one hand to prove that only one path starts from each point of the corresponding domain, and on the other hand to characterize the analytic expression of boundaries.

In order to cover the first quadrant we have selected one special path for each of the nine different kinds of path of the sufficient family; by symmetry all other domains may be obtained.

In the following we construct these domains, one by one, in P_θ. For each kind of path, integrating successively the differential system on the time intervals during which (u_1, u_2) is constant, we obtain the parametric expression of initial points. In each case we obtain the analytical expression of boundaries; computations are tedious but quite easy (a more detailed proof is given in [33]).

We do not describe here the construction of all domains. We just give a detailed account of the computation of the first domain, the eight other domains are constructed exactly the same way. Figure 9 presents the covering of the first quadrant in $P_{-\frac{\pi}{4}}$, the different domains are represented.

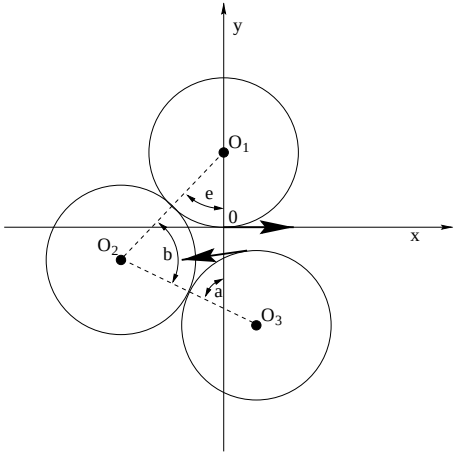

Fig. 7. Path $l_a^+ l_b^- l_e^+$

Construction of domain of path $C|C|C$: As we said in the introductive section, Sussmann and Tang have shown that the study of family $C|C|C$ may be restricted to paths types $l^+l^-l^+$ and $r^+r^-r^+$. As we only consider values of θ in $[-\pi, 0]$ it suffice to study the type $l_a^+ l_b^- l_e^+$ (figure 7). By lemma 15, a, b and e are positive real numbers verifying: $0 \leq a + b + e \leq \pi$.

Along this trajectories the control (u_1, u_2) takes successively the values $(+1, +1), (-1, +1)$ and $(+1, +1)$. By integrating the system (4) for each of these successive constant values of u_1 and u_2, from the initial configuration (x, y, θ) to the final configuration $(0, 0, 0)$ we get:

$$\begin{cases} x = \sin\theta + 2\sin(b+e) - 2\sin e \\ y = -\cos\theta + 2\cos(b+e) - 2\cos e + 1 \\ \theta = -a - b - e \end{cases} \tag{23}$$

Let us now consider that the value of θ is fixed. The arclength parameter e varies in $[0, -\theta]$; given a value of e, b varies in $[0, -\theta - e]$. When e is fixed as b varies, the initial point traces an arc of the circle ζ_e of radius 2 centered at $P_e(\sin\theta + 2\sin e, -\cos\theta - 2\cos e + 1)$

One end point of this arc is the point $E(\sin\theta, -\cos\theta + 1)$ (when $b = 0$), depending on the value of e the other end point (corresponding to $b = -\theta - e$) describes an arc of circle of radius 2 centered at the point $H(-\sin\theta, \cos\theta + 1)$ and delimited by the point E (when $e = -\theta$) and its symmetric F with respect to the origin O (when $e = 0$).

For different values of e the arcs of ζ_e make a foliation of the domain; this ensures the existence of a unique trajectory of this type starting form every

point of the domain. Figure (8) represents this construction for two different values of θ. The cross section of this domain appears at figure (9) with the eight other domains making the covering of the first quadrant in $P_{-\frac{\pi}{4}}$.

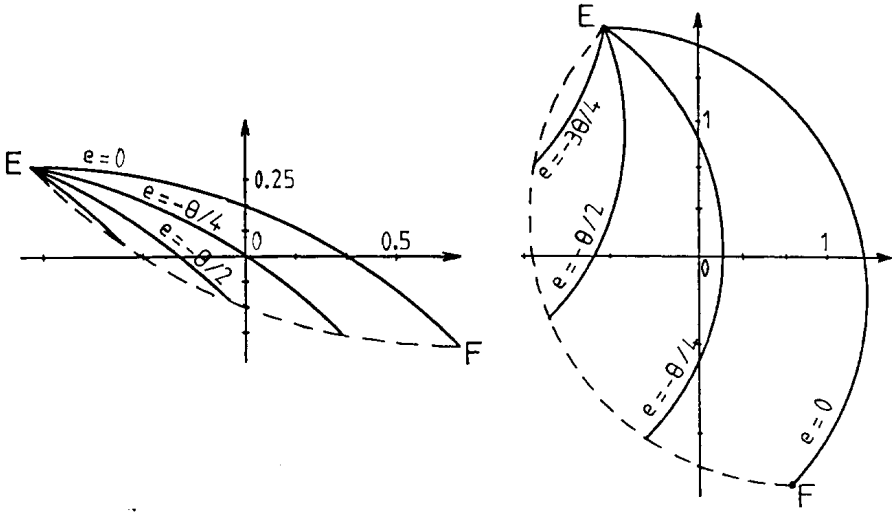

Fig. 8. Cross section of the domain of path $l_a^+ l_b^- l_e^+$ in P_θ, ($\theta = -\frac{\pi}{4}$ left side) and ($\theta = -\frac{3\pi}{4}$ right side).

- As this domain is symmetric about the two axes Δ_θ and $\Delta_\theta^\perp$, it follows from lemma 12 that the domain of path $l^- l^+ l^-$ is exactly the same one. This point corroborates the result by Sussmann and Tang which states that the search for an optimal path of the family $C|C|C$ (when $\theta \leq 0$) may be limited to one of these two path types.
- When $\theta = -\pi$ the domain is the disc of radius 2 centered at the origin.

Following the same method the eight other domains are easily computed (see [33]), they are represented at figure 9 in the plane $P_{-\frac{\pi}{4}}$. The domain's boundaries are piecewise smooth curves of simple sort: arcs of circle, line segments, arcs of conchoids of circle or arcs of cardioids.

Analysis of the construction As we know exactly the equations of the piecewise smooth boundary curves, we can precisely describe the domains in each plane P_θ. This construction insures the complete covering of the first

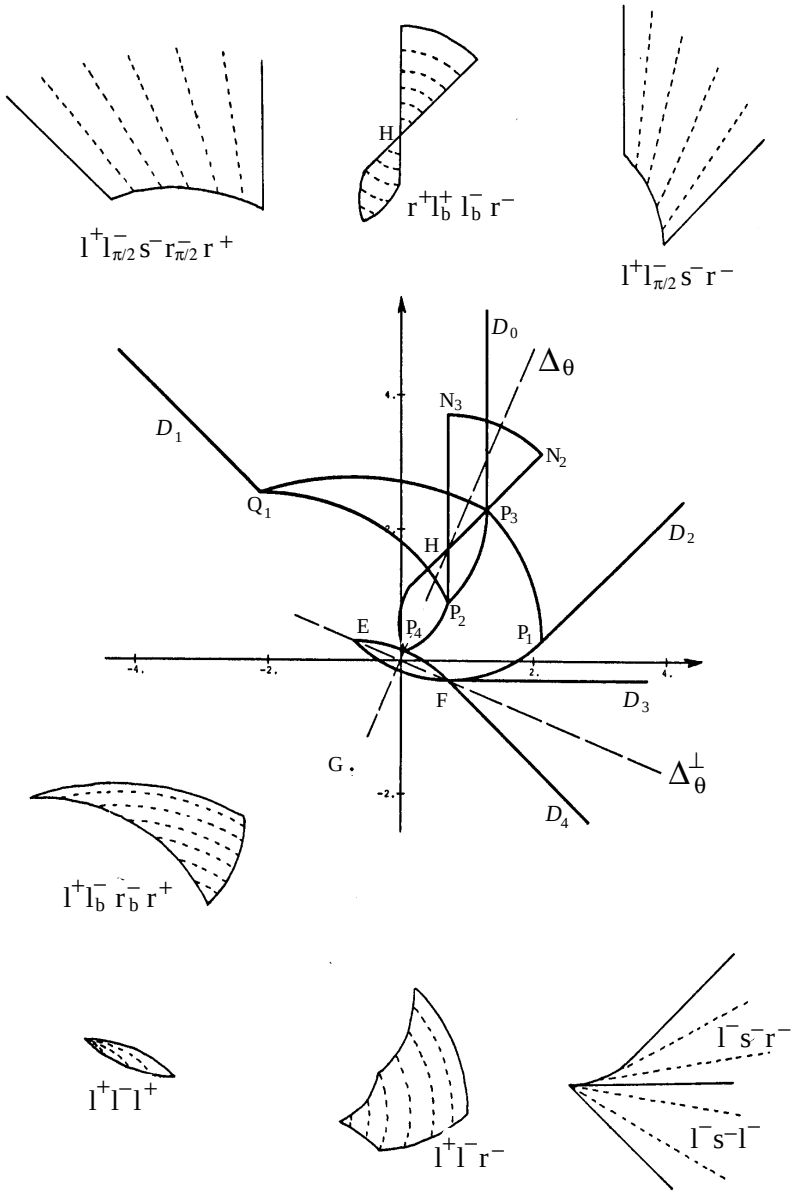

Fig. 9. The various domains covering the first quadrant in $P_{-\frac{\pi}{4}}$ (foliations appear in dotted line).

quadrant, and by symmetry the covering of the whole plane. All types in the sufficient family are represented[3]. Analysing the covering of the first quadrant, we can note that almost all the domains are adjacent, describing a continuous variation of the path shape. Nevertheless some domains overlap and others are not wholly contained in the first quadrant. Therefore, if we consider the covering of the whole plane (see fig 10), many intersections appear. In a region belonging to more than one domain, several paths are defined, and finding the shortest one will require a deeper study. At first sight, the analysis of all intersections seems to be combinatorially complex and tedious, but we will show that some geometric arguments may greatly simplify the problem. First, let us consider the following remarks about the domains covering the first quadrant:

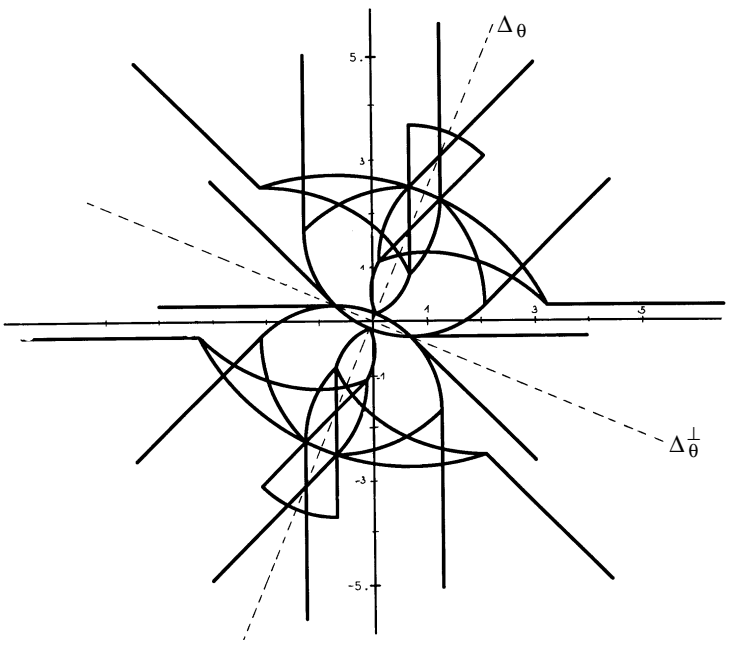

Fig. 10. Overlapping of domains covering the plane $P_{-\frac{\pi}{4}}$.

– Except for the domain $r^+l^+l^-r^-$, all domains are adjacent two-by-two (i.e. they only have some parts of their boundary in common). Then, inside

[3] However, each domain is only defined for θ belonging to a subset of $[-\pi, \pi]$. So in a given plane P_θ only the domains corresponding to a subfamily of family (22) refined by lemma 15 appear.

the first quadrant we only have to study the intersection of the domain $r^+l^+l^-r^-$ with the neighbouring domains.

– Some domains are not wholly contained in the first quadrant, therefore, they may intersect domains covering other quadrants. Nevertheless, among the domains overlapping other quadrants, some are symmetric about Δ_θ or $\Delta_\theta^\perp$. These domains are:
  - the domains $l^+l^-l^+$ and $r^+l^+l^-r^-$ symmetric about Δ_θ,
  - the domains $l^+l^-l^+$ and $l^-s^-l^-$ symmetric about $\Delta_\theta^\perp$, (i.e. all domains intersecting $\Delta_\theta^\perp$.)

  In this case, we consider that only one half of the domain belongs to the covering of first quadrant. Therefore, no intersections may occur with the symmetric domains.

Finally, we only have to study two kinds of intersections: on the one hand the intersections of pairs of symmetric domains with respect to Δ_θ, (section 3), and on the other hand the intersections inside the first quadrant between the domain $r^+l_b^+l_b^-r^-$ and the neighbouring domains (section 3).

Refinement of domains intersecting Δ_θ In this section we prove that the path $l^+l^-r^-$, $l^+l_b^-r_b^-r^+$, $l^+l_{\frac{\pi}{2}}^-s^-r_{\frac{\pi}{2}}^-r^+$, and $l^+l_{\frac{\pi}{2}}^-s^-r^-$, stop being optimal as soon as their projections in P_θ cross the Δ_θ-axis. This will allow us to remove the part of these domains lying out of the first quadrant.

1/ Path $l^+l^-r^-$

Lemma 16. A path $l^+l^-r^-$ linking a directed point $(M(x,y),\theta)$ to $(0,0,0)$, with $y > -x\cot\frac{\theta}{2}$, is never optimal.

Proof: Suppose that there is a path $\mathcal{T}_1$ of type $l^+l^-r^-$ from a directed point $(M_1(x_1,y_1),\theta_1)$ to $(0,0,0)$, verifying $y_1 > -x_1\cot\frac{\theta_1}{2}$. Let M_2 be the cusp point (Figure 11). M_2 is such that [4] $y_2 < -x_2\cot\frac{\theta_2}{2}$. Let us consider a directed point (M,θ) moving along the path from (M_1,θ_1) to (M_2,θ_2). As M moves, the direction θ increases continuously from θ_1 to θ_2. As a result, the corresponding line Δ_θ varies from Δ_{θ_1} to Δ_{θ_2}. Its slope increases continuously from $-\cot\frac{\theta_1}{2}$ to $-\cot\frac{\theta_2}{2}$. Then, by continuity, there exists a directed point (M_α,α) on the arc (M_1,M_2), verifying $y_\alpha = -x_\alpha\cot\frac{\alpha}{2}$. From lemma 12, there exist two isometric paths of type $l^+l^-r^-$ and $r^+l^+l^-$ linking (M_α,α) to the origin. Thus, (M_1,θ_1) is linked to the origin by a path of type $l^+r^+l^+l^-$ having the same length as $\mathcal{T}_1$. Such a path violates both necessary conditions **A** and **B** of PMP (lemma 11): (**A:** D_0 and D^+ cannot be parallel) and (**B:** u_2 is not constant). As a consequence, $\mathcal{T}_1$ is not optimal. □

[4] This assertion can be easily deduced from the construction of the domain of path $l^-s^-r^-$.

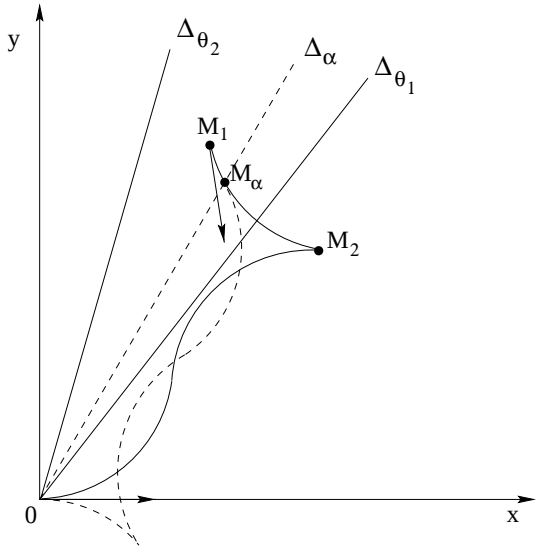

Fig. 11. There exists a point M_α such that $M_\alpha \in \Delta_\alpha$.

2/ Path $l^+ l^-_{\frac{\pi}{2}} s^- r^-$

The shape of this path is close to the shape of the path $l^+_a l^-_b r^-_e$ ($b = \frac{\pi}{2}$ and a line segment is inserted between the last two arcs). Then, we can use exactly the same reasoning to prove the following lemma:

Lemma 17. A path $l^+ l^-_{\frac{\pi}{2}} s r^-$ linking a directed point $(M(x,y),\theta)$ to $(0,0,0)$, with $y > -x \cot \frac{\theta}{2}$, is never optimal.

3/ Path $l^+ l^-_b r^-_b r^+$

Lemma 18. A path $l^+ l^-_b r^-_b r^+$ linking a directed point $(M(x,y),\theta)$ to $(0,0,0)$, with $y > -x \cot \frac{\theta}{2}$, is never optimal.

Proof: The reasoning is the same as in the proof of lemma 16. Assume that there is a path $\mathcal{T}_1$ of type $l^+ l^-_b r^-_b r^+$ linking a directed point $(M_1(x_1,y_1),\theta_1)$, verifying $y_1 > -x_1 \cot \frac{\theta_1}{2}$, to $(0,0,0)$. Let M_2 be the cusp-point; the subpath of $\mathcal{T}_1$ from (M_2,θ_1) to the origin is of the type $l^- r^- r^+$ symmetric to the type treated in Lemma 16. Therefore, the coordinates of M_2 must verify $y_2 < -x_2 \cot \frac{\theta_2}{2}$. Now, let us consider a directed point (M,θ) moving along the arc from (M_1,θ_1) to (M_2,θ). With the same arguments as in the proof of Lemma 16, there exists a directed point (M_α,α) on this arc, with $\theta_1 \leq \alpha \leq \theta_2$, verifying $y_\alpha = -x_\alpha \cot \frac{\alpha}{2}$. From lemma 12, there exist two

isometric paths of types $l^+l_b^-r_b^-r^+$ and $r^-r_b^+l_b^+l^-$ linking (M_α, α) to the origin. As a result, (M_1, θ_1) is linked to the origin by a path of the type $l^+r^-r_b^+l_b^+l^-$ having the same length as $\mathcal{T}_1$. This path is not optimal because the robot goes twice through the same configuration; therefore $\mathcal{T}_1$ cannot be optimal. □

4/ Path $l^+l_{\frac{\pi}{2}}^-s^-r_{\frac{\pi}{2}}^-r^+$

The shape of this path is close to the shape of the path $l^+l_b^-r_b^-r^+$ ($b = -\frac{\pi}{2}$ and a line segment is inserted between the two middle arcs). Then, we can use exactly the same arguments to prove the next lemma.

Lemma 19. A path $l^+l_{\frac{\pi}{2}}^-s^-r_{\frac{\pi}{2}}^-r^+$ linking a directed point $(M(x,y),\theta)$ to $(0,0,0)$, with $y > -x\cot\frac{\theta}{2}$, is never optimal.

Now, with lemmas 16 to 19 we can remove the part of domains $l^+l^-r^-$, $l^+l_{\frac{\pi}{2}}^-s^-r^-$, $l^+l^-r^-r^+$ and $l^+l_{\frac{\pi}{2}}^-s^-r_{\frac{\pi}{2}}^-r^+$ lying out of the first quadrant (on the other side of Δ_θ). Moreover, according to the analyse made at section 4.3, we only have to consider, the half part of the domains symmetric about Δ_θ or $\Delta_\theta^\perp$ located in the first quadrant. As every domain intersecting $\Delta_\theta^\perp$ is symmetric about this axis, we can construct the covering of all other quadrants without generating new intersections. Inside each quadrant, it remains to study the intersection between the domain of path $C|C_bC_b|C$ and the neighbouring domains. Once again we restrict ourselves to the first quadrant.

Intersections inside the first quadrant From the construction of domains covering the first quadrant, it appears that the domain $r^+l_b^+l_b^-r^-$ may intersect the following three adjacent domains: $l^+l_{b'}^-r_{b'}^-r^+$, $l^+l_{\frac{\pi}{2}}^-s^-r_{\frac{\pi}{2}}^-r^+$ and $l^+l_{\frac{\pi}{2}}^-s^-r^-$. Furthermore the intersection between the domain $r^+l_b^+l_b^-r^-$ and the domains $l^+l_{\frac{\pi}{2}}^-s^-r_{\frac{\pi}{2}}^-r^+$ and $l^+l_{\frac{\pi}{2}}^-s^-r^-$ only happens when b is strictly greater than $\frac{\pi}{3}$. First, as a corollary of lemma 16, we are going to prove that a path $r^+l_b^+l_b^-r^-$ is never optimal when $b > \frac{\pi}{3}$. Therefore the corresponding part of this domain will be removed and the intersections of domains inside the first quadrant will be reduced to the overlapping of domains $r^+l_b^+l_b^-r^-$ and $l^+l_{b'}^-r_{b'}^-r^+$.

Corollary 1. A path of the family $CC_b|C_bC$ verifying $b > \frac{\pi}{3}$ cannot be optimal.

Proof: Let us consider a path of the type $r_a^+l_b^+l_b^-r_e^-$. If this path is optimal, then the subpath $l_b^+l_b^-r_e^-$ is also optimal. Integrating the corresponding system we obtain the expression of initial points coordinates:

$$\begin{cases} x = \sin\theta - 2\sin(e-b) + 2\sin e \\ y = -\cos\theta + 2\cos(e-b) - 2\cos e + 1 \end{cases}$$

with $\theta = e - 2b$ (since the first two arcs of circles have the same length) and from lemma 16 the coordinates must verify $y \leq -\cot\frac{\theta}{2}x$. Replacing x and y by their parametric expression, we obtain after computation:

$$\sin\frac{e}{2}(2\cos b - 1) \geq 0 \quad \text{then} \quad b \leq \frac{\pi}{3} \quad (\text{since} \quad 0 < e \leq \frac{\pi}{2}\ ) \quad \square$$

Therefore according to the previous construction we may remove the part of the domain $r^+l_b^+l_b^-r^-$ located beyond the point H with respect to O. (see figure 9).

Now, only one intersection remains inside the first quadrant, between the domains $r_a^+l_b^+l_b^-r_e^-$ and $l_{a'}^+l_{b'}^-r_{b'}^-r_{e'}^+$; let us call $\mathcal{I}$ this region. In order to determine which paths are optimal in this region, we compute in each plane P_θ the set of points that may be linked to the origin by a path of each kind having the same length. Initial point of these two paths are respectively defined by the following parametric systems:

$$(r_a^+l_b^+l_b^-r_e^-)\ \begin{cases} x = -\sin\theta + 2(2\cos b - 1)\sin(e-b) \\ y = \cos\theta - 2(2\cos b - 1)\cos(e-b) + 1 \end{cases}$$

$$(l_{a'}^+l_{b'}^-r_{b'}^-r_{e'}^+)\ \begin{cases} x = \sin\theta - 4\sin e' + 2\sin(e'+b') \\ y = -\cos\theta + 4\cos e' - 2\cos(e'+b') - 1 \end{cases} \tag{24}$$

the length of these paths are respectively:

$$\begin{cases} L = a + 2b + e = 4b + \theta \text{ with } \theta = e - 2b + a \\ L' = e' + 2b' + a' = 2(b'+e') - \theta \text{ with } \theta = e' - a' \end{cases} \tag{25}$$

The required condition $L = L'$ implies that $\theta + 2b - b' - e' = 0$. By replacing $e' + b'$ by $\theta + 2b$ in the second system, then writing that both systems are equivalent we obtain:

$$\begin{cases} \sin(e-b)(1-2\cos b) + \sin\theta - 2\sin e' + \sin(\theta+2b) = 0 \\ \cos(e-b)(1-2\cos b) + \cos\theta - 2\cos e' + \cos(\theta+2b) + 1 = 0 \end{cases}$$

we eliminate the parameter e' writing that $\sin^2(e') + \cos^2(e') = 1$; then after computation, we obtain the following relation between e and b:

$$4\cos^2 b - 2\cos b + (1 - 2\cos b)(2\cos(e - 2b - \theta)\cos b + \cos(e-b)) + \cos\theta + \cos(\theta + 2b) - 1 = 0 \tag{26}$$

As $e - 2b - \theta = e - b - (b + \theta)$, this equation may be rewritten as follows:

$$A\sin(e-b)+B\cos(e-b)+C=0$$

where A, B and C are functions of b and θ defined by:

$$\begin{cases} A = 2(1-2\cos b)\sin(b+\theta)\cos b \\ B = (1-2\cos b)(2\cos(b+\theta)\cos b+1) \\ C = 4\cos^2 b - 2\cos b + \cos\theta + \cos(\theta+2b) - 1 \end{cases}$$

Therefore we can express $\sin(e-b)$ and $\cos(e-b)$ by solving a second degree equation; we obtain:

$$\sin(e-b) = \frac{-AC \pm |B|\sqrt{A^2+B^2-C^2}}{A^2+B^2} \tag{27}$$

The discriminant $\mathcal{D} = A^2+B^2-C^2$ may be factored as follows:

$$\mathcal{D} = 4\cos(b)\sin^2(\frac{b+\theta}{2})(\cos(2b+\theta)+\cos(\theta)+6\cos(b)-4)$$

therefore, as $b \in [0, \frac{\pi}{3}]$, the sign of $\mathcal{D}$ is equal to the sign of

$$E(b) = \cos(2b+\theta)+\cos(\theta)+6\cos(b)-4$$

Let us call $b_{\max}$ the value of b solution of $E(b)=0$. As E(b) is a decreasing function of b, E(b) is positive when $b \leq b_{\max}$. We will see later that the maximal value of b we have to consider verifies this condition, ensuring our problem to be well defined.

Now, as the region $\mathcal{I}$ is delimited by the vertical line (P_2, N_3), each point belonging to $\mathcal{I}$ must verify: $x \leq \sin\theta$. Moreover, as the type $r^+l_b^+l_b^-r^-$ is defined for $b \in [-\theta, \frac{\pi}{3}]$, we can deduce from the first line of system (24) that $\sin(e-b)$ is negative. As a result, the choice of the positive value of the discriminant in (27) cannot be a solution of our problem. From this condition we determine a unique expression for $\sin(e-b)$ and $\cos(e-b)$. Replacing these expressions in system (24) we obtain the parametric equation of a curve γ_θ issued from P_2 (when $b=-\theta$), dividing the region $\mathcal{I}$ into two subdomains, and crossing the axis Δ_θ at a point T (see figure 12). The value b_T of b corresponding to the point T may be characterized in the following manner:

From lemma 12 we know that any path of type $r_a^+l_b^+l_b^-r_e^-$ starting on Δ_θ verifies $a=e$; it follows that $e-b-\frac{\theta}{2}=0$. Replacing $e-b$ by $\frac{\theta}{2}$ in (26) b_T appears as being the solution of the implicit relation $R(b)=0$, where:

$$R(b) = 4\cos^2 b - 2\cos b + (1 - 2\cos b)(2\cos(b + \frac{\theta}{2})\cos b + \cos\frac{\theta}{2}) + \cos\theta + \cos(\theta + 2b) - 1 \quad (28)$$

Now, combining the relation $R(b_T) = 0$ with the expression of $E(b_T)$ we can prove simply that $b_T \leq b_{\max}$ in order to insure the sense of our result. Therefore, R(b) being a decreasing function of b, the values of $b \in [-\theta, b_T]$ are the values of $b \in [-\theta, \frac{\pi}{3}]$ verifying $R(b) \geq 0$. The curve γ_θ is the only set of points in $\mathcal{I}$ where both paths have the same length. As the distance induced by the shortest path is a continuous function of the state, this curve is the real limit of optimality between these two domains. This last construction achieves the partition of the first quadrant, and by the way the partition of the whole plane.

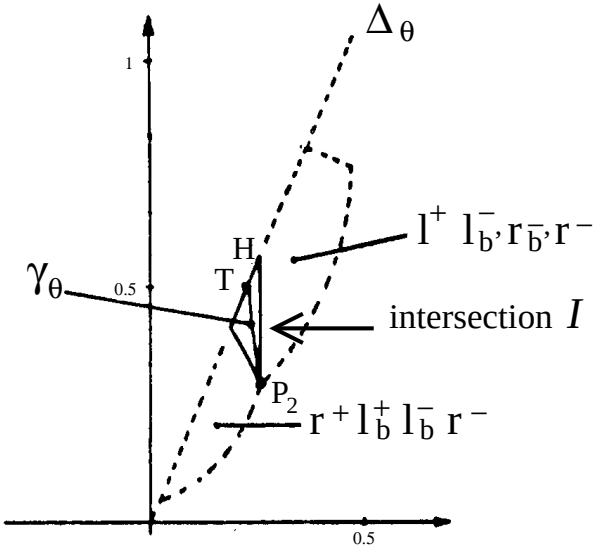

Fig. 12. The curve γ_θ splitting the intersection of domains $r^+ l_b^+ l_b^- r^-$ and $l^+ l_{b'}^- r_{b'}^- r^-$ in the first quadrant of $P_{-\frac{\pi}{4}}$

Description of the partition Figures (13),(14) and (15) show the partition of the plane P_θ for several values of θ all these pictures have been traced from the

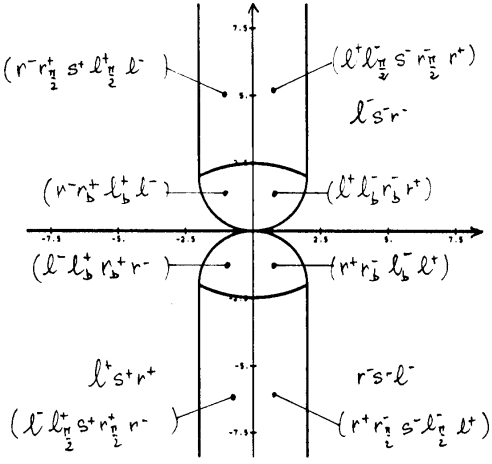

$\theta = 0$

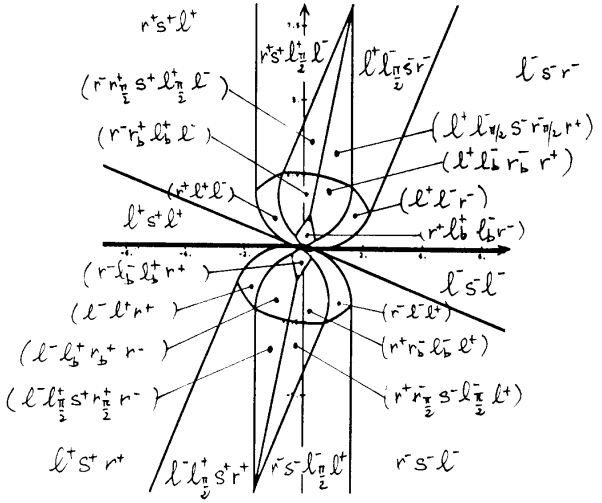

$\theta = -\frac{\pi}{8}$

Fig. 13. Partitions of planes P_0 and $P_{-\frac{\pi}{8}}$

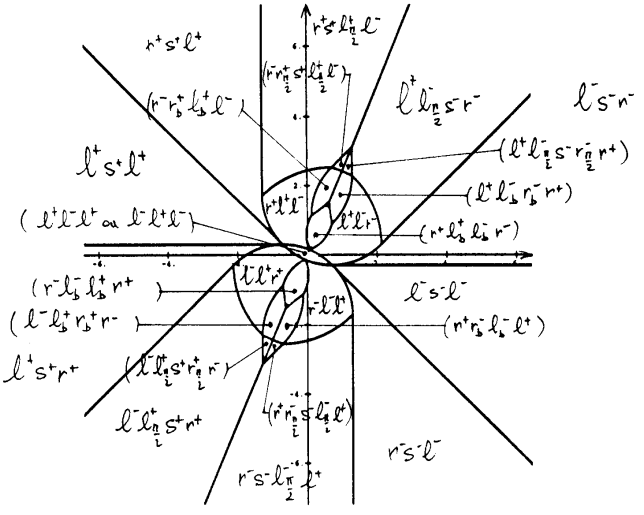

$\theta = -\frac{\pi}{4}$

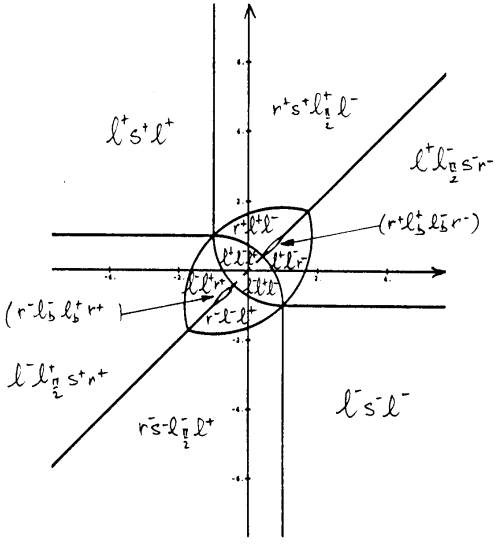

$\theta = -\frac{\pi}{2}$

Fig. 14. Partitions of planes $P_{-\frac{\pi}{4}}$ and $P_{-\frac{\pi}{2}}$

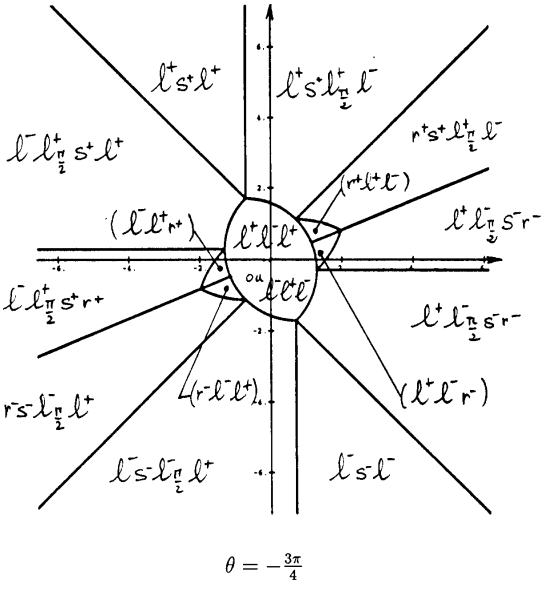

Fig. 15. Partitions of planes $P_{-\frac{3\pi}{4}}$ and $P_{\pm\pi}$

analytical equations of boundaries by using the symbolic computation software *Mathematica*. Each elementary cell consists of directed points that may be linked to the origin by the same kind of optimal path. The 46 domains never appear together in a plane P_θ; the following table presents the values of θ for which each domain exists[5]

Type	*Intervals of validity*
$CC_u\|C_uC$	$[-\frac{2\pi}{3}, 0]$ and $[0, \frac{2\pi}{3}]$
$C\|C_uC_u\|C$	$[-\frac{\pi}{3}, \frac{\pi}{3}]$
$C\|CC$ and $CC\|C$	$[-\pi, 0]$ and $[0, \pi]$
$C\|C_{\frac{\pi}{2}}SC$ and $CSC_{\frac{\pi}{2}}\|C$ if $sign(u_2)$ changes	$[-\pi, 0]$ and $[0, \pi]$
$C\|C_{\frac{\pi}{2}}SC$ and $CSC_{\frac{\pi}{2}}\|C$ if $sign(u_2)$ is constant	$[-\pi, -\frac{\pi}{2}]$ and $[\frac{\pi}{2}, \pi]$
$C\|C\|C$	$[-\pi, 0]$ and $[0, \pi]$
CSC if $sign(u_2)$ changes	$[-\frac{\pi}{2}, \frac{\pi}{2}]$
CSC if $sign(u_2)$ is constant	$[-\pi, 0]$ and $[0, \pi]$
$C\|C_{\frac{\pi}{2}}SC_{\frac{\pi}{2}}\|C$	$[-2\ \mathrm{arccot}(2), 2\ \mathrm{arccot}(2)]$

When θ varies in $[-\pi, \pi]$ the partition of planes P_θ induces a partition of $\mathbf{R}^2 \times [-\pi, \pi]$. Identifying the planes $P_{-\pi}$ and P_π we obtain a partition of the configuration space $\mathbf{R}^2 \times S^1$.

In most part of domains the optimal solution is uniquely determined. However, there exist some regions of the space where several equivalent path are defined. To describe these regions we introduce the following notation.

In the first quadrant of each plane P_θ, we denote by Δ_θ^T the half-line defined as the part of Δ_θ located beyond the point T (with respect to O). According to lemmas 16 to 19, paths $l^+l^-r^-$, $l^+l^-_{\frac{\pi}{2}}s^-r^-$, $l^+l^-_br^-_br^+$, and $l^+l_{\frac{\pi}{2}}s^-r^-_{\frac{\pi}{2}}r^+$ stop being optimal as soon as they cross Δ_θ^T, but are still optimal on Δ_θ^T. As the same reasoning holds for the domains symmetric with respect to Δ_θ, there exist two equivalent paths optimal for linking any point of Δ_θ^T to the origin. The same phenomenon occurs on the curve γ_θ where paths $r^+l^+_bl^-_br^-$ and $l^+l^-_br^-_br^+$ have the same length. Hence, in the first quadrant, two equivalent paths are defined at each point of $\Delta_\theta^T \cup \gamma_\theta$. By symmetry with respect to Δ_θ and $\Delta_\theta^\perp$, we can define such a set inside the four other quadrants. Let us call N_θ the union of these four symmetric sets.

At any point of $P_\theta \setminus N_\theta = \{p \in P_\theta,\ p \notin N_\theta\}$ a unique path is defined if $\theta \not\equiv \pi\ mod(2\pi)$. Inside each domain the uniqueness is proven by the existence of

[5] These values of θ have been deduced from the bounds on the parameters given by the partition. Details are given in [34].

a foliation, and on the boundaries (outside N_θ) any path is defined as a continuous transition between two types (and belongs to both path types). However, according to lemma 14, when $\theta \equiv \pi \; mod(2\pi)$, two equivalent (isometric) paths are defined at any point of $P_\theta \setminus N_\theta$ and therefore, four equivalent paths are defined at any point of N_θ. As we have seen in the construction, there always exist two equivalent paths ($l^+l^-l^+$ and $l^-l^+l^-$ when $\theta > 0$) and ($r^+r^-r^+$ and $r^-r^+r^-$ when $\theta < 0$) linking any point of the central domain $C|C|C$ to the origin. Furthermore, when the initial orientation θ equals $\pm\pi$, there exist two equivalent strategies for linking any point of the plane to the origin, each one corresponding to a different direction of rotation of the point (see lemma 14). In that case each of the four paths $C|C|C$ is optimal in the central disc of radius 2.

By choosing one particular solution in each region where several optimal path are defined, one can determine a synthesis of optimal paths according to definition 7. Therefore, the determination of such a synthesis is not unique.

In each cross section P_θ, the synthesis provides a complete analytic description of the boundary of domains which appear to be of simple sort: line segment, arc of circle, arc of cardioid of circle, etc. Therefore, to characterize an optimal control law for steering a point to the origin, it suffice to determine in which cell the point is located, without having to do further test. This provides a complete solution to Reeds and Shepp's problem.

On the other hand, this study constitutes an interesting way to focus on the insufficiency of a local method, such as Pontriagyn's maximum principle, for solving this kind of problem. The Δ_θ axis appeared as a boundary and we had to remove the piece of domains lying on one side of this axis. More precisely, we have shown that any trajectory stops being optimal as it crosses the set N_θ. This phenomenon is due to the existence of several wavefronts intersecting each other on this set. For this reason two equivalent paths are defined at each point of N_θ. (each of them corresponds to a different wave front). PMP is a local reasoning based on the comparison of each trajectory with the trajectories obtained by infinitesimally perturbating the control law at each time. As this reasoning cannot be of some help to compare trajectories belonging to different wave fronts, it is necessary to use a geometric method to conclude the study, as we did in section 3 and 3. The main problem remains to determine *a priori* the locus of points where different wave fronts intersect.

The construction we have done for determining a partition of the phase space required a complex geometric reasoning. In the following section we will show how Boltianskii's verification theorem can be applied *a posteriori* to provide a simple new proof of this result.

4.4 An example of regular synthesis

In this section, we prove that the previous partition effects a regular synthesis in any open neighbourhood of O in $\mathbf{R}^2 \times S^1$. First of all, we need to prove that the curves and surfaces making up the partition define piecewise smooth sets. From the previous construction we know that the restriction of any domain to planes P_θ is a connected region delimited by a piecewise smooth boundary curve. Except for the curve γ_θ (computed at section 3) each smooth component $\mathcal{C}_i(\theta)$ of the boundary remains a part of a same geometric figure $\mathcal{F}$ (line, circle, conchoid of circle, ...) as θ varies. Let $M^i(\theta)$ and $N^i(\theta)$ be the extremities of the curve $\mathcal{C}_i(\theta)$. As θ varies, the position and orientation of $\mathcal{F}$ as well as the coordinates of $M^i(\theta)$ and $N^i(\theta)$ vary as smooth functions of θ. Therefore, in $\mathbf{R}^2 \times [-\pi, \pi]$, the lines trace smooth ruled surfaces, and the circles and conchoids draw smooth surfaces. In each case we have verified that the boundary curves $M^i(\theta)$ and $N^i(\theta)$ of these surfaces never connect tangentially, making sure that all these surfaces are non singular 2-dimensional smooth surfaces.

The study of the surface Γ, made up by the union of the horizontal curves γ_θ when θ varies in $[-\frac{\pi}{3}, \frac{\pi}{3}]$ requires more attention. As γ_θ is the region of P_θ where paths $r_a^+ l_b^+ l_b^- r_e^-$ and $l_a^+ l_b^- r_b^- r_e^+$ have the same length, the surface Γ is defined as the image of the set $D_\Gamma = \{(\theta, b) \in \mathbf{R}^2, \theta \in [-\frac{\pi}{3}, 0], b \in [-\theta, b_T]\}$ by the following mapping:

$$\begin{cases} x = -\sin\theta + 2(2\cos b - 1)\sin(e - b) \\ y = \cos\theta - 2(2\cos b - 1)\cos(e - b) + 1 \\ \theta = e - 2b + a \end{cases}$$

where $\sin(e - b)$ and $\cos(e - b)$ are deduced from formula (27) and b_T is the solution of the implicit equation $R(b) = 0$ where $R(b)$ is given by (28).

Using the symbolic computation software *Mathematica* we have checked that the matrix of partial derivatives has full rank 2 at each point of D_Γ. Therefore, as the domain D_Γ is a 2-dimensional region of the plane (θ, b) without singularities, delimited by two smooth curves, Γ constitutes a 2-dimensional smooth surface (see figure 16).

All the pieces of surfaces, making up the partition are 2-dimensional smooth surfaces and from remark 4 we know that they constitute 2-dimensional piecewise-smooth sets. If P^2 is the union of these surfaces, P^1 the union of their smooth boundary curves $M^i(\theta)$ and $N^i(\theta)$, P^0 the target point O, then in any open neighbourhood $\mathcal{V}$ of O we can write the required relation: $P^0 \subset P^1 \subset P^2 \subset \mathcal{V}$.

In order to check the regularity conditions we have considered each trajectory one-by-one. following the representative point from the initial point to the origin we have analysed the different cells encountered. We have checked that the cell's dimension varies according to the hypothesis **B** of definition 9. In each case we have verified that the point never reaches the next cell tangentially. For

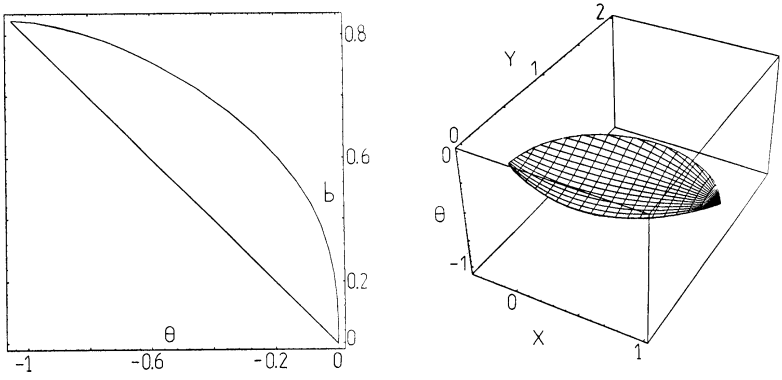

Fig. 16. Set D_Γ (left) and surface Γ (right)

each trajectory we can represent this study within a table by describing from the top to the bottom the cells σ_i successively crossed. Each cell corresponds to a subpath type represented by a subword of the initial word. In each case we specify the dimension and the type (T_1) or (T_2) of the cells encountered. When the point passes from a cell σ_i to a cell $\Pi(\sigma_i) = \sigma_{i+1}$ we verify that the trajectory riches σ_{i+1} with a nonzero angle α_i. This is done by comparing the vector $\boldsymbol{v}_i$ tangent to the trajectory with a vector $\boldsymbol{n}_{i+1}$ normal to σ_{i+1} (if σ_{i+1} is a 2-dim cell), or with a vector $\boldsymbol{w}_{i+1}$ tangent to σ_{i+1} (if σ_{i+1} is a 1-dim cell). In any case the last cell, described in the bottom of the table, is a 1-dimensional cell which is a piece of trajectory linking the point to P_0.

Due to the lack of place we just present here the table corresponding to paths $l_a^+ l_{\frac{\pi}{2}}^- s_d^- r_{\frac{\pi}{2}}^- r_e^+$, an exhaustive description of all path types may be found in [35].

Path $l_a^+ l_{\frac{\pi}{2}}^- s_d^- r_{\frac{\pi}{2}}^- r_e^+$					
Cell	Dim	Type	$\boldsymbol{v}_i$	$\boldsymbol{n}_i$ or $\boldsymbol{w}_i$	angle α_i
$\sigma_1 : l_a^+ l_{\frac{\pi}{2}}^- s_d^- r_{\frac{\pi}{2}}^- r_e^+$	3	T_1	$\boldsymbol{v}_1 \begin{pmatrix} \cos\theta \\ \sin\theta \\ 1 \end{pmatrix}$		
$\sigma_2 : l_{\frac{\pi}{2}}^- s_d^- r_{\frac{\pi}{2}}^- r_e^+$	2	T_2		$\boldsymbol{n}_2 \begin{pmatrix} \cos\theta \\ \sin\theta \\ 3+d \end{pmatrix}$	$\boldsymbol{n}_2.\boldsymbol{v}_1 = d+4 \neq 0$ because $d > 0$ then $\alpha_2 \neq 0$
$\sigma_3 : l_b^- s_d^- r_{\frac{\pi}{2}}^- r_e^+$	3	T_1	$\boldsymbol{v}_3 \begin{pmatrix} -\cos\theta \\ -\sin\theta \\ 1 \end{pmatrix}$		
$\sigma_4 : s_d^- r_{\frac{\pi}{2}}^- r_e^+$	2	T_1	$\boldsymbol{v}_4 \begin{pmatrix} -\cos\theta \\ -\sin\theta \\ 0 \end{pmatrix}$	$\boldsymbol{n}_4 \begin{pmatrix} \sin\theta \\ -\cos\theta \\ 2+d \end{pmatrix}$	$\boldsymbol{n}_4.\boldsymbol{v}_3 = 2+d \neq 0$ because $d > 0$ then $\alpha_4 \neq 0$
$\sigma_5 : r_{\frac{\pi}{2}}^- r_e^+$	1	T_2		$\boldsymbol{w}_5 \begin{pmatrix} \cos\theta - 2\sin\theta \\ \sin\theta + 2\cos\theta \\ 1 \end{pmatrix}$	$\boldsymbol{v}_4$ and $\boldsymbol{w}_5$ not colinear then $\alpha_5 \neq 0$
$\sigma_6 : r_k^- r_e^+$	2	T_1	$\boldsymbol{v}_6 \begin{pmatrix} -\cos\theta \\ -\sin\theta \\ -1 \end{pmatrix}$		
$\sigma_7 : r_e^+$	1	T_1		$\boldsymbol{w}_7 \begin{pmatrix} \cos\theta \\ \sin\theta \\ -1 \end{pmatrix}$	$\boldsymbol{v}_6$ and $\boldsymbol{w}_7$ not colinear then $\alpha_7 \neq 0$

Now, let us analyse carefully the other regularity conditions: Let N be the set defined by $N = \cup_{\theta \in [-\pi,\pi]} N_\theta$ where N_θ is the set defined at section 3 as the union of γ_θ, Δ_θ^T and their image by the axial symmetries with respect to Δ_θ and $\Delta_\theta^\perp$. From the previous reasoning we know that N is a piecewise smooth set. Let v be the function defined in $\mathcal{V}$, taking its values in the control set $U = \{(u_1, u_2), |u_1| = 1, \text{and } u_2 \in [-1, 1]\}$ which defines an optimal control law at each point. In each cell where more than one optimal solution exists the choice of a constant control has been done in order to define the function v in a unique way.

A - As stated in the beginning of this section, all the i-dim cells are i-dimensional smooth manifolds. Moreover, as each cell corresponds to a same path type, the control function v takes a constant value at each point of the cell. Therefore, v is obviously continuously differentiable inside each cell, and may be prolonged into an other constant function when the point reaches the next cell.

B - All the 3-dim cells are of type T_1

- When the representative point passes from a cell to another it never arrives tangentially. Furthermore, as $u_1 = 1$, the velocity never vanishes.

- Along the trajectory, the variation of cell types (T_1) or (T_2) follows the rule stated by Boltianskii.

C - Along any trajectory, the representative point pierces at most three cells of type T_2 and reaches the point O after a finite time.

D - From every point of N there start two trajectories having the same length and from any point of $\mathcal{V} \setminus N$ there issues a unique trajectory.

E - All these trajectories satisfy the necessary conditions of PMP.

F - By crossing a border (except the set N) from a domain to another, either the length of one elementary piece making up the trajectory vanishes, or a new piece appears. When the point crosses the set N, the optimal strategy switches suddenly for an isometric trajectory. Therefore, in any case, the path length is a continuous function of the state in $\mathcal{V}$ (see [26] for more details).

With this conditions the function v and the sets P_i effect a regular synthesis in $\mathcal{V}$. As the point moves with a constant velocity, it is equivalent to minimize the path length or the time, we have $f^0(x,u) \equiv 1$. Finally, as the coordinate functions $f^1(x,u) = \cos\theta u_1$, $f^2(x,u) = \sin\theta u_1$ and $f^3(x,u) = u_2$ have continuous partial derivatives in x and u, the hypotheses of theorem 6 are verified providing a new proof of our preceding result.

To our knowledge, this construction constitutes the first example of a regular synthesis for a nonholonomic system in a 3-dimensional space.

5 Shortest paths for Dubins' Car

Let us now present more succinctly the construction of a synthesis of optimal paths for Dubins' problem (DU). This results is the fruit of a collaboration between the project *Prisme* of INRIA Sophia Antipolis and the group *Robotics and Artificial Intelligence* of LAAS-CNRS see [10] for more details.

At first sight, this problem might appear as a subproblem of RS. Nevertheless, the lack of symmetry of the system, due to the impossibility for the car to move backwards, induces strong new difficulties. Nevertheless, the method we use for solving this problem is very close to the one developed in the preceding section.

The work is based on the sufficient family of trajectories determined by Dubins (14). Note that this sufficient family can also be derived from PMP (see [36]). The study is organized as before. First, we determine the symmetry properties of the system and we use them to reduce the state space and to refine Dubins' sufficient family. Then, in a second time we construct the domains corresponding to each path type and we analyse their intersections. As we did in studying the problem RS, we consider the restriction of domains to planes P_θ where the orientation θ is constant.

Remark 10. *As Dubins' car only moves forwards its more convenient to fix the initial configuration of the car to be at the origin* $(O, 0)$ *of the space, and to search for the configuration* (M, θ) *reachable from this point.*

5.1 Symmetry and reduction properties

As the linear velocity u_1 is fixed to 1 we can rewrite system 2 as follows:

$$\begin{cases} \dot{x} = \cos\theta \\ \dot{y} = \sin\theta \\ \dot{\theta} = u \end{cases} \tag{29}$$

where $u \in [-1, 1]$ represents the angular velocity. In the study of Reeds and Shepp's problem we have shown that it was possible to construct several isometric trajectories by using simple geometric arguments. Nevertheless, as system (29) is no more symmetric, these properties are not valid for Dubins' problem. In particular, if $\mathcal{T}$ is a trajectory admissible for DU, the trajectory symmetric to $\mathcal{T}$ with respect to the point O is no more admissible. Therefore, the sole symmetry property that remains valid for DU, is the existence of isometric trajectories ending at points symmetric with respect to $\Delta_\theta^\perp$ in each plane P_θ. This result can be easily proven by using the same reasoning as the one developed in the proof of lemma 12. We use the notations introduced for the study of Reeds and Shepp's problem.

Lemma 20. In the plane of the car's motion (O, x, y) let (M, θ) be a configuration of the car and M^3 the point symmetric to M with respect to $\Delta_\theta^\perp$. If $\mathcal{T}$ is a trajectory admissible for DU starting at the origin $(O, 0)$ and ending at (M, θ), there exists another admissible trajectory $\mathcal{T}^3$ isometric to $\mathcal{T}$ which links the origin to the configuration (M^3, θ).

As for RS the word describing $\mathcal{T}^3$ is obtained by reversing the word describing $\mathcal{T}$. On the other hand, the symmetry with respect to the x-axis provides another isometric admissible trajectory as follows:

Lemma 21. If $\mathcal{T}$ is an admissible trajectory for DU, starting at the origin and ending at $(M(x, y), \theta)$, there exists another admissible trajectory $\overline{\mathcal{T}}$ isometric to $\mathcal{T}$, which starts at the origin and ends at $(\overline{M}(x, -y), -\theta)$.

Dubins' sufficient family (14) contains two path types:

- $C_a S_d C_e$ with $a, e \in [0, 2\pi[$ and $d \geq 0$,
- $C_a C_b C_e$ with $a, e \in [0, 2\pi[$ and $b \in]\pi, 2\pi[$.

From lemma 20, we can restrict our study to paths: lrl, rlr, rsr, lsl and either rsl or lsr. Furthermore thanks to lemma 21 we only have to consider the values of θ such that a representative of their class modulo 2π belongs to $[0, \pi]$. Let us now state three lemmas providing additional necessary optimality conditions.

Lemma 22. A necessary condition for a path $C_a C_b C_e$ to be optimal is that:

$$\begin{cases} \pi < b < 2\pi \\ 0 \leq a \leq b \text{ and } 0 \leq e \leq b \\ 0 \leq a < b - \pi \text{ or } 0 \leq e < b - \pi \end{cases}$$

Proof: The first condition on b has been already given by Dubins [16] or in [2,36]. A characteristic straight line D_0 is defined for each optimal path (as in lemma 11), which supports line segments and where inflection points occur. On one side of this line the path turns clockwise, and on the other side, counterclockwise. Thus if $a > b$ (resp. $e > b$), the first (resp. last) arc must cross the line D_0; this is not possible.

For the last condition, suppose that the contrary is true: $a \geq b - \pi$ and $e \geq b - \pi$. Consider the circle tangent to both extremal arcs. Tracing an arc of this new circle we can build a shorter path as follows (see figure 17): an arc shortened to length $a - b + \pi$ on the first circle, concatenated to an arc of length $2\pi - b$ on the new circle followed by an arc of length $e - b + \pi$ on the last circle.□

Lemma 23. Paths rsr (*resp.* lsl) such that the sum of the length of the two arcs of circle is equal to 2π can be replaced by an isometric path lsl (*resp.* rsr).

Proof: It suffice to consider figure 18. Whenever there exists a path of type $r_a s_d r_e$ (resp. $l_a s_d l_e$) with $a + e = 2\pi$ there also exists an equivalent path $l_e s_d l_a$ (resp. $r_e s_d r_a$) □

Lemma 24. Along any optimal trajectory the maximal variation of θ is 2π.

Proof:

- Types rsl and lsr: As the directions of rotation on each arcs are opposite and the length of each arc is lower or equal to 2π, the result follows.
- From lemma 22, on types $r_a l_b r_e$ and $l_a r_b l_e$ the arclength verify: $0 \leq a \leq b$ and $0 \leq e \leq b$. therefore $|a - e + b| \leq v < 2\pi$.
- Types rsr and lsl: Suppose that the initial and final orientations are equal. From lemma 23 we know that in the case that $a + e = 2\pi$, if a path of type $r_a s_d r_e$ (resp. $l_a s_d l_e$) exists, there also exists an equivalent path of type $l_e s_d l_a$ (resp. $r_e s_d r_a$). It follows that a path $r_a s_d r_e$ (resp. $l_a s_d l_e$) with $a + e = 2\pi + \epsilon$ cannot be optimal because it is equivalent to a path $l_e s_d l_a r_\epsilon$ which does not verify the necessary conditions of PMP (points of inflection and line segment must belong to the same line D_0). □

Now, taking into account these new bounds on arclength, and the symmetry properties we construct the domains corresponding to each path type in planes P_θ.

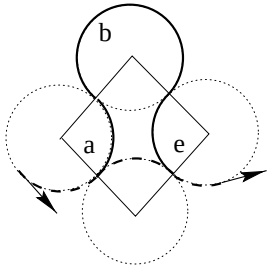

Fig. 17. Non optimal $C_aC_bC_e$ trajectory

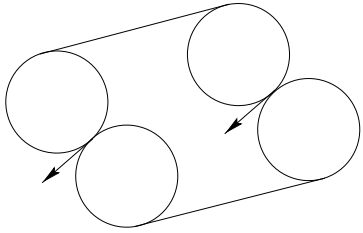

Fig. 18. Simultaneous existence of path r_asr_e and l_esl_a when $a + e = 2\pi$

5.2 Construction of domains

From lemma 20 it suffice to construct the domains of paths lsl, rsr, lsr, rlr and lrl. The domain of path rsl will be obtained from the domain of path lsr by symmetry with respect to the $\Delta_\theta^\perp$-axis.

From lemma 24 we know that the final orientation $\theta \in S^1$ may be viewed as a real number belonging to $[-2\pi, 2\pi]$. Therefore, according to lemma 21 and lemma 23, we only have to consider the cross sections of domains belonging to planes P_θ with $\theta \in [0, \pi]$ or $\theta + 2\pi \in [0, \pi]$.

Integrating the differential system (29) for the successive constant values of the input u (as we did for RS in section 4.3) we compute the cross section of each domain. We do not give here the detail of the construction (see [11]). To describe the construction we need to introduce the following notations.

- E is the point of coordinates $(\sin\theta, 1 - \cos\theta)$,
- G is the point of coordinates $(\sin\theta, -1 - \cos\theta)$,
- F (*resp.* H) is the point symmetric to E (*resp.* G) w.r.t. the origin O,
- J (*resp.* K) is the point symmetric to H (*resp.* G) w.r.t. point E,
- $\mathcal{D}_0$ (*resp.* $\mathcal{D}_1$) is the ray from E towards positive x-coordinates, of orientation 0 (*resp.* θ),
- $\mathcal{D}_2$ (*resp.* $\mathcal{D}_3$) is the ray from F parallel to $\mathcal{D}_0$ (*resp.* $\mathcal{D}_1$),
- we denote by $\mathcal{C}_P$ the circle (or the disc) centered at the generic point P and with radius 2.

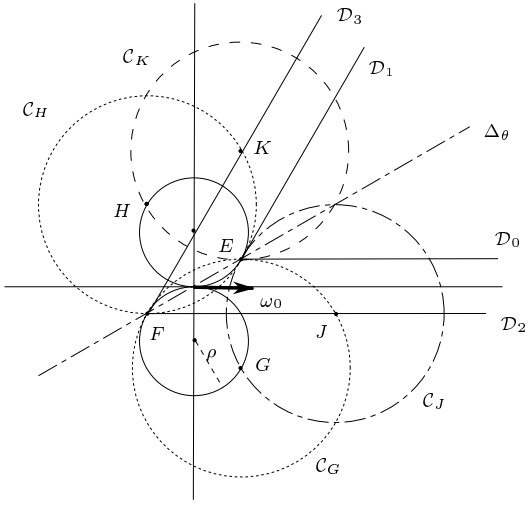

Fig. 19. Particular points, lines and circles

Then we have:

- the lsl domain is the internal angular sector defined by $\mathcal{D}_0$ and $\mathcal{D}_1$,
- the rsr domain is the external angular sector defined by $\mathcal{D}_2$ and $\mathcal{D}_3$,
- the rsl domain is the exterior of circle $\mathcal{C}_G$,
- the lrl domain is the union of the intersections between the pairs of discs $\mathcal{C}_G$ and $\mathcal{C}_H$, $\mathcal{C}_G$ and $\mathcal{C}_J$, $\mathcal{C}_H$ and $\mathcal{C}_K$,
- the rlr domain is the union of discs $\mathcal{C}_G$ and $\mathcal{C}_H$.

Notice that these domains intersect each other and do not partition P_θ. Each domain is defined upon two parameters. By fixing one parameter as the other one varies, we trace iso-parametric curves creating a foliation of each domain. From this construction it appears that a unique path of each type starts from each point located in the interior of the domain.

5.3 Construction of the partition

At this stage, we have to determine which path type is actually optimal in each region of P_θ covered by more than one domain. We are sure of the optimality of the whole lsl domain for the lsl type, even if other domains intersect it. Indeed, this domain is optimal for RS, and Dubins' sufficient family is included in the Reeds and Shepp one (except for CCC paths, which are shortened by $C|C|C$ paths). Clearly, a path type with no cusp which is optimal for RS is a fortiori optimal for DU.

So, let us consider the other intersections. Due to the lack of the symmetry with respect to the Δ_θ-axis, we cannot use a geometric reasoning to compare isometric trajectories, as we did in section 3 for RS. Therefore, in each region where more than one path type occur (see fig. 19), we use the method developed at section 3 for RS to compute the boundaries of the subdomains in which each path type is optimal. This method is based on the computation of the set of points reachable by a path of each type having the same length and starting at the origin. We conclude with arguments of continuity based on the foliation of domains by iso-length curves.

We will only present here the final equations of these boundary curves, since the calculation are really tedious (see [11] for more details).

Intersection *rsr* / *rsl* The intersection of these two domains, is defined by the complementary in P_θ to the set made by the union of the disc $\mathcal{C}_G$ and the internal angular sector defined by the rays $\mathcal{D}_2$ and $\mathcal{D}_3$. Writing that the final point are identical, and that both curves have the same length, we get a system of three equations with four variables. Fixing one variable as a parameter, we obtain the parametric expression of a curve $\mathcal{I}_0$:

$$\mathcal{I}_0 \quad \begin{cases} x = \lambda \cos a + 2 \sin a + \sin\theta \\ y = -\lambda \sin a + 2 \cos a - \cos\theta - 1 \end{cases}$$

where $\lambda = \frac{\rho(a+\theta-\pi)^2+2(\cos(a+\theta)-1)}{\sin(a+\theta)-(a+\theta-\pi)}$, and a is the length of the first arc in the rsl path. This parameter varies within the interval $]\pi-\theta, \mu]$ for $\theta \in [0, \pi[$ where μ is defined as follows:

- for $\theta \leq \frac{\pi}{2} + \pi$, $\mu = \pi - \theta + \eta$ where η is the solution of the non-algebraic equation $\cos t = t$,
- for $\theta \geq \frac{\pi}{2} + \pi$, μ is the value of a obtained when $\mathcal{I}_0$ and $\mathcal{D}_2$ intersect. This value can be computed by equating the parametric system of both curves.

This curve divides the region of intersection into two sub-domains, and admits the line of orientation θ, passing through G, as asymptote. We define the symmetric curve $\mathcal{I}_1$ for the intersection between rsr and lsr.

Intersection *rsl* / *lsr* Let η defined as in section 5.3. For $\theta \leq \frac{\pi}{2} + \eta$ we deduce from the analysis of iso-distance curves of each type that lsr paths are always shorter than rsl paths in the infinite region delimited by $\mathcal{D}_1$, $\mathcal{D}_3$, and the arc (E, K) of circle $\mathcal{C}_H$. Symmetrically with respect to the $\Delta_\theta^\perp$- axis, in the infinite region delimited by $\mathcal{D}_0$, $\mathcal{D}_2$, and the arc (E, J) of circle $\mathcal{C}_G$ the paths rsl are shorter than the lsr ones.

For $\theta > \frac{\pi}{2} + \pi$ a new boundary curve $\mathcal{I}_6$ appears; it is the locus of points reachable from the origin by a path rsl and lsr having the same length. This

curve is determined by equating the parametric system of both curves. The curve $\mathcal{I}_7$ is obtained by symmetry with respect to $\Delta_\theta^\perp$ (see fig. 24)

Intersection *rsr / rlr* This region of intersection is made up by the parts of the discs $\mathcal{C}_G$ and $\mathcal{C}_H$ lying inside the external angular sector defined by $\mathcal{D}_2$ and $\mathcal{D}_3$. We find geometrically that the set of points reachable from the origin by a path of each type rsr and rlr having the same length belongs to a circle called $\mathcal{I}_2$ of radius 4η and centered at F. Thus, this set is made of two arcs of the circle $\mathcal{I}_2$ respectively defined by the interval of polar angles: $[\max(\theta, \pi/2 - \eta), \min(\theta, \pi/2 + \eta)]$ and the symmetric interval w.r.t. $\theta/2$. This intersection only occurs if $\theta \leq \pi/2 + \eta$.

Intersection *rlr / lrl* Using the same reasoning as in the study of the first intersection, we deduce that inside the region determined by the union of the intersections of discs $\mathcal{C}_G$ and $\mathcal{C}_J$, and the intersection of discs $\mathcal{C}_H$ and $\mathcal{C}_K$, rlr paths are always shorter than lrl paths. However, for $\theta > \pi/2$, the region of intersection of discs $\mathcal{C}_G$ and $\mathcal{C}_H$ is divided into two subdomains by a curve called $\mathcal{I}_3$. Paths rlr are optimal in the first subdomain, whereas paths lrl are optimal in the other one.

After a change of variables, due to the rotation of angle $\theta/2$, we obtain the following parametric equations for $\mathcal{I}_3$:

$$\mathcal{I}_3 \begin{cases} X = \dfrac{\cos v + \cos(v+\theta)}{\sin\frac{\theta}{2}} \\ Y^2 = (4\ \sin\frac{v}{2})^2 - (X - 2\sin\frac{\theta}{2})^2 \end{cases}$$

where v is the length of the middle arc of the lrl path. See [11] for the detail relative to the determination of the interval in which v varies.

Intersection *rlr / rsl* This last intersection occurs in the region of the disc $\mathcal{C}_H$ located outside the disc $\mathcal{C}_G$ and inside the internal angular sector delimited by $\mathcal{D}_2$ and $\mathcal{D}_3$. Using the same method as before we determine a curve $\mathcal{I}_4$ delimiting two subdomains in which rlr and rsl are respectively optimal . The curve $\mathcal{I}_5$ symmetric of $\mathcal{I}_4$ with respect to $\Delta_\theta^\perp$ determines the boundary between the subdomains of paths rlr and lsr in the symmetric region. The parametric

equations of $\mathcal{I}_4$ are:

$$\mathcal{I}_4 \begin{cases} x = 2\,(\,\sigma\cos a + \sin a\,) + \sin\theta \\ y = 2\,(\,\sigma\sin a - \cos a\,) - \cos\theta - 1 \end{cases}$$

$$\begin{aligned} \text{with } a &= 2\pi - \arccos\alpha \\ \alpha &= \frac{\sigma^2\,A + B\,\sqrt{4\,(1+\cos\sigma)^2 + 4\,(\sigma+\sin\sigma)^2 - \sigma^4}}{2\,(A^2+B^2)} \\ A &= \cos\theta\,(1+\cos\sigma) - \sin\theta\,(\sigma+\sin\sigma) \\ B &= \cos\theta\,(\sigma+\sin\sigma) + \sin\theta\,(1+\cos\sigma) \end{aligned}$$

where a is the length of the first arc and 2σ the length of the line segment in the rsl path. We can notice that, here again, equations are non-algebraic. This intersection only occurs for $\theta \geq \pi/2 - \eta$. See [11] for the determination of the range of σ.

5.4 Description of the partition

With the refinement provided by the previous section we finally obtain a partition of P_θ, for values of θ having a representative modulus 2π in $[0, \pi]$. Using the symmetry properties given by lemmas 20 and 21 we obtain the partition for any $\theta \in S^1$. The shape of domains varies continuously with respect to θ. In the sequel we describe four successive states of the partition according to four successive intervals of θ. We also describe the cross sections corresponding to two particular values: $\theta = 0$ and π:

- $\theta = 0$ (Figure 20)
  All the domains are represented but notice that, for three of them, not only one but two equivalent optimal paths are defined at each point. Notice also that, in fact, the lrl and lsl domains are not connected: the initial configuration O can be viewed as a point of the domain lrl (isolated in P_0), and the horizontal half-line $(x \geq 0, y = 0)$ also belongs to the domain lsl.
- $\theta \in]0, \pi/2 - \eta]$ (Figure 21)
  For $\theta \neq 0$, a unique path type is defined in each domain, but some domains are not connected (rlr, rsl and lsr). For $\theta = \pi/2 - \eta$, the segment of $\mathcal{D}_2$ (*resp.* $\mathcal{D}_3$) and $\mathcal{I}_2$ intersect each other on $\mathcal{C}_{G}$ (*resp.* $\mathcal{C}_{H}$).
- $\theta \in]\pi/2 - \eta, \pi/2]$ (Figure 22)
  Here, the intersection curves $\mathcal{I}_4$ and $\mathcal{I}_5$ appear, and for $\theta = \pi/2$ the two crescents of the rlr domain are connected at one point on the $\Delta_{\pi/2}$ axis.
- $\theta \in]\pi/2, \pi/2 + \eta]$ (Figure 23)
  The intersection curve $\mathcal{I}_3$ has appeared between rlr and lrl. Everything varies continuously until $\mathcal{I}_2$ disappear when $\theta = \pi/2 + \eta$, since the segment of $\mathcal{D}_2$ (*resp.* $\mathcal{D}_3$), $\mathcal{I}_4$ (*resp.* $\mathcal{I}_5$), $\mathcal{I}_0$ (*resp.* $\mathcal{I}_1$) and the circle $\mathcal{C}_{G}$ (*resp.* $\mathcal{C}_{H}$) are concurrent.

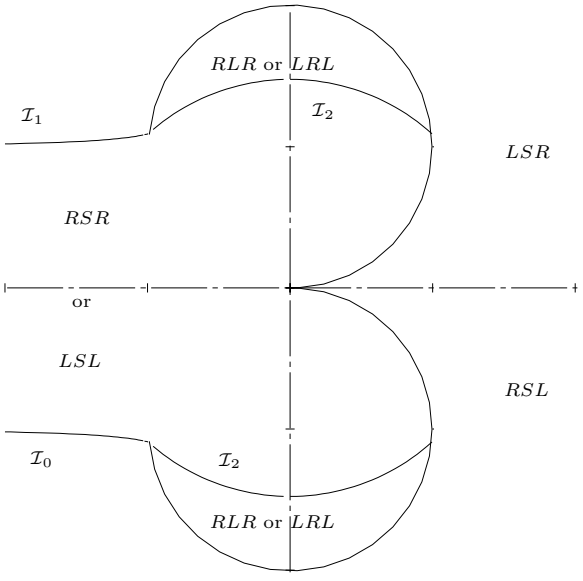

Fig. 20. Partition of P_0

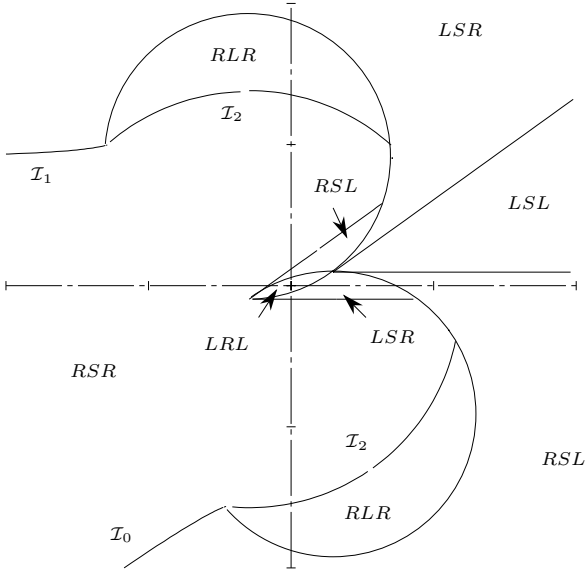

Fig. 21. Partition of $P_{\frac{\pi}{5}}$

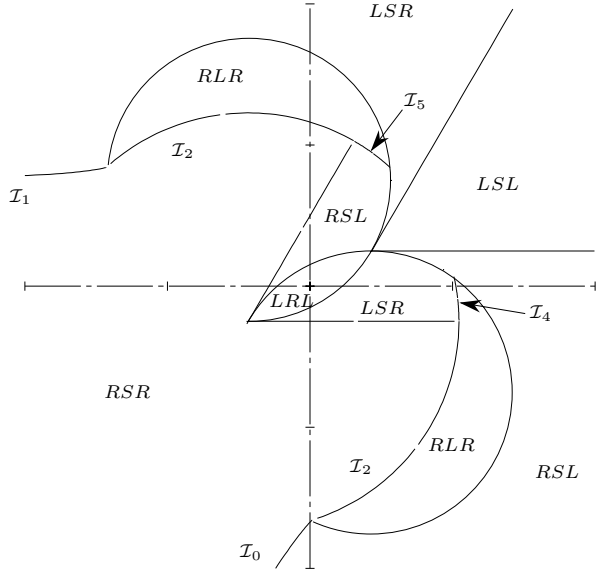

Fig. 22. Partition of $P_{\frac{\pi}{3}}$

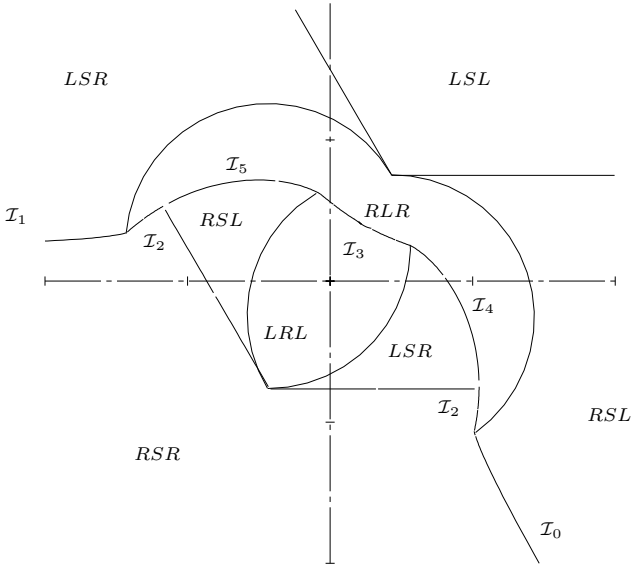

Fig. 23. Partition of $P_{\frac{2\pi}{3}}$

– $\theta \in]\pi/2 + \eta, \pi[$ (Figure 24)
Domains are still varying continuously until $\mathcal{I}_4$ and $\mathcal{I}_5$ disappear, $\mathcal{I}_4$ and $\mathcal{I}_5$ become horizontal half-lines, and $\mathcal{I}_3$ becomes an horizontal segment of length 4.

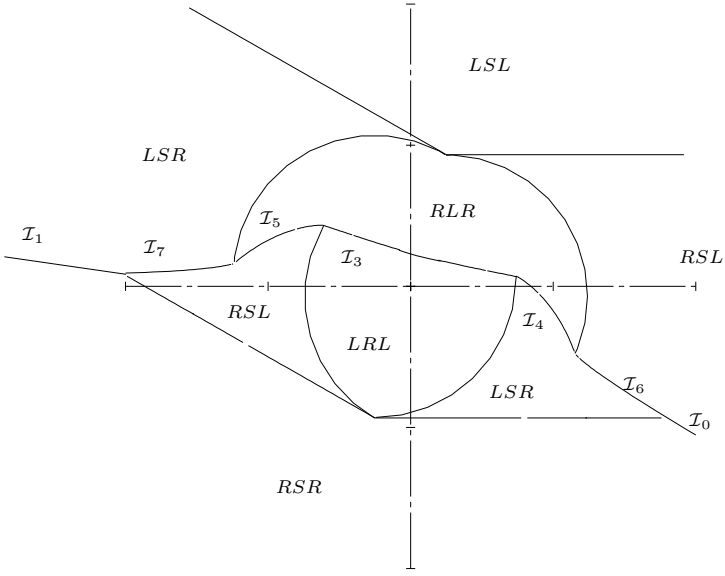

Fig. 24. Partition of $P_{\frac{5\pi}{6}}$

– $\theta = \pi$ (Figure 25)
In this case the partition contains six types; the domains of paths lsr and rsl are still not connected.

Analysing this construction we can make the following remarks:

1. Optimal domains are not necessarily connected, unlike the Reeds and Shepp case. This is due to the fact that a configuration (x, y, θ) can sometimes be reached in different ways: either mostly turning left until the algebraic sum of angles equals θ, or mostly turning right so that the algebraic sum equals $2\pi - \theta$. For the Reeds and Shepp case, these two solutions cannot be both optimal since the algebraic sum of angles has to be lower than π.
2. The shape of the shortest paths varies continuously when crossing the boundary of any domain, except the boundary arcs of discs $\mathcal{C}_G$ and $\mathcal{C}_H$, and the intersection curves $\mathcal{I}_i$.

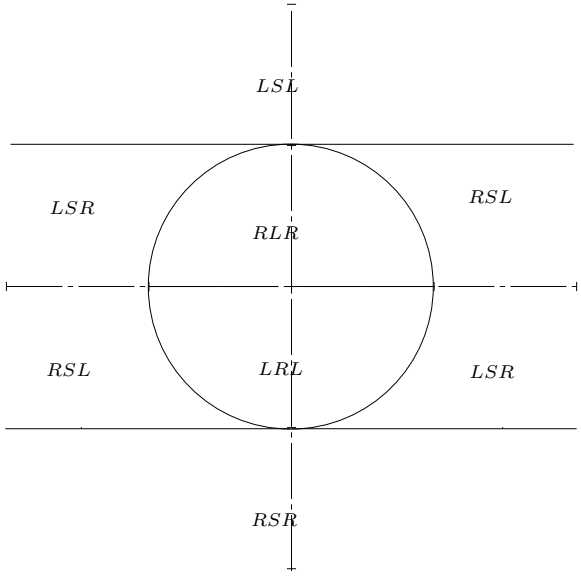

Fig. 25. Partition of P_π

3. The shortest path's length is a continuous function of (x, y, θ) everywhere, *except* on the boundary arcs of discs $\mathcal{C}_{_G}$ and $\mathcal{C}_{_H}$. This discontinuity (in shape and length) is due to the fact that inside the circle $\mathcal{C}_{_G}$ (*resp.* $\mathcal{C}_{_H}$) the rsl (*resp.* lsr) path does not exist. Figure 26 represents the iso-distance curves in the plane P_θ for $\theta = 1$ *rad*. The two thicker arcs in the center of the picture represent the locus of points where the length function is discontinuous.
4. For $\theta = 0$, there exist two regions where two equivalent optimal solution are defined. Therefore, to define a synthesis of optimal paths (uniqueness of the solution), it suffice to choose arbitrarily a constant values for the control in each region where several optimal strategies are available.

Remark 11. *Due to the lack of continuity of the length function, this synthesis of optimal paths does not verify Boltianskii's regularity conditions (condition F of definition 9 fails). This illustrates the fact that the very strong hypotheses defining Boltianskii's regular synthesis restrict the application area to a very small class of problems. This example raises up the interest of searching for sufficient conditions, weaker than Bolitanskii's ones, that still guarantee the optimality of marked trajectories.*

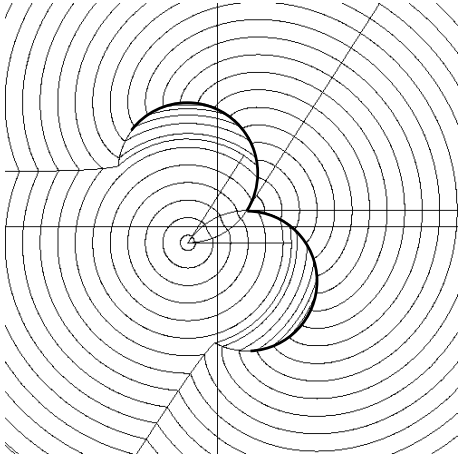

Fig. 26. Iso-distance curves in P_1 and discontinuity of the length function.

5.5 Related works

Using also the frame of geometric control, R. Felipe Monroy Pérez has studied Dubins' problem in the case of Euclidean and non-Euclidean geometries [28].

In the Euclidean case (classical problem of Dubins) he provided a new proof of the non optimality of the concatenation of four arcs of circle. He proved that in two dimensional simply connected manifold with constant sectional curvature, trajectories of minimal length necessarily follow Dubin's pattern (CLC and CCC) where L denotes a piece of a geodesic and C an arc of curve with constant curvature. The study was done by means of optimal control on Lie groups.

For the three dimensional case, he exhibited an explicit expression of the torsion of optimal arcs. In particular, he determined a parametric equation of curves satisfying optimality conditions in $\mathbf{R}^3$, providing a representation of potential solutions for Dubins' problem in $\mathbf{R}^3$.

Dubins' problem in $\mathbf{R}^3$ has been also studied by H. J. Sussmann in [37]. By applying PMP on manifolds he proved that every minimizer is either an helicoidal arc or a path of the form CSC or CCC.

6 Dubins model with inertial control law

From the previous section we know that optimal solutions of Dubins' problem are sequences of line segments and arcs of circle of minimal radius. Therefore, there exist curvature discontinuities between two successive pieces, line-arc or

arc-arc (with opposite direction of rotation) and to follow (exactly) such a trajectory a real robot would be constrained to stop at the end of each piece. In order to avoid this problem, Boissonnat, Cerezo and Leblond [3] have proposed a generalization of Dubins' problem by suggesting to control the angular acceleration of the car instead of its angular velocity. This section presents the analysis of the shortest paths problem for this model.

Using the same notation as for Dubins' problem, let $M(x, y)$ be the coordinates of the robot's reference point with respect to a fixed orthonormal frame, and θ its orientation with respect to the $x-$axis. We use $\kappa(t)$ to represent the signed curvature of the path at each time ($\kappa(t) > 0$, meaning that the car is turning left).

In the plane of the robot's motion we consider a class $\mathcal{C}$ of C^2 paths joining two given configurations $X_0 = (M_0, \theta_0, \kappa_0)$ and $X_f = (M_f, \theta_f, \kappa_f)$.

Definition 11. *A path belongs to class $\mathcal{C}$ if it satisfies the following two properties:*

1. Regularity: *the path is a C^2 concatenation of an at most countable number of open C^3 arcs of finite length, and the set of endpoints of these arcs, also called the* switching points*, admits at most a finite number of accumulation points.*
2. Constraint: *along the path, the absolute value of the derivative of the curvature , with respect to the arc length, is upper bounded by a given constant $B > 0$, at every point where it is defined.*

With these notations and the above definition, the motion of the oriented point $M(t) = (x(t), y(t), \theta(t), \kappa(t))$ along paths of class $\mathcal{C}$ in $\mathbf{R}^2 \times S^1 \times \mathbf{R}$ is well-defined and continuous.

In the sequel we consider that the robot moves at constant speed 1, so that time and arc length coincide.

A path in class $\mathcal{C}$ between any two configurations $X_0 = (x_0, y_0, \theta_0, \kappa_0)$ and $X_f = (x_f, y_f, \theta_f, \kappa_f)$, if it exists, is entirely determined by the function $v(t) = \dot{\kappa}(t)$, defined and continuous everywhere, except at the switching points, by the following differential system:

$$\dot{X}(t) = \begin{cases} \dot{x}(t) = \cos\theta(t) \\ \dot{y}(t) = \sin\theta(t) \\ \dot{\theta}(t) = \kappa(t) \\ \dot{\kappa}(t) = v(t) \end{cases} \tag{30}$$

If we add the boundary conditions $X(0) = X_0$, $X(f) = X_f$, and the constraint:

$$\forall t \in [0, T], \quad |v(t)| \leq B, \tag{31}$$

and if we search for a path of minimum length in class $\mathcal{C}$, we have turned the geometric problem into a classical question of optimal control theory where the functional:

$$J(v) = T = \int_0^T dt \tag{32}$$

is to be minimized among the set of control functions v satisfying (31).

6.1 Existence of an optimal solution

System (30) may be written as:

$$\dot{X} = F(X, v) = f(X) + v\, g(X)\,,$$

where the analytic vector fields f and g are given by:

$$f(X) = \begin{pmatrix} \cos\theta \\ \sin\theta \\ \kappa \\ 0 \end{pmatrix} \;,\; g(X) = \begin{pmatrix} 0 \\ 0 \\ 0 \\ 1 \end{pmatrix} .$$

Complete controllability of the system We first observe that the Lie algebra $\mathcal{L}(f, g)$ generated by f and g is, at each point, of dimension 4. Indeed, $\forall X \in \mathbf{R}^4$,

$$h(X) = [g, f](X) = \begin{pmatrix} 0 \\ 0 \\ 1 \\ 0 \end{pmatrix} \;,\; i(X) = [h, f](X) = \begin{pmatrix} -\sin\theta \\ \cos\theta \\ 0 \\ 0 \end{pmatrix} ,$$

and

$$\det \begin{bmatrix} \cos\theta & 0 & 0 & -\sin\theta \\ \sin\theta & 0 & 0 & \cos\theta \\ \kappa & 0 & 1 & 0 \\ 0 & 1 & 0 & 0 \end{bmatrix} = -1\,.$$

Moreover, the solutions of the associated autonomous system $\dot{X} = f(X)$ are circles (of radius $1/\kappa$), thus periodic. Hence, Bonnard's theorem [27, thm.III.4] applies, to establish the complete controllability of (30) under the constraint (31). This means that any X_0 and X_f can always be joined by a path satisfying (30) and (31).

Existence of an optimal control The existence of an optimal control for the problem (30), (31), (32), with given X_0 and X_f, is ensured by Fillipov's existence theorem (see [13, 5.1.ii] for example). Indeed, the hypotheses of the theorem are satisfied. The dynamic $F(X, v)$ and the cost $J(v)$ are smooth enough, the set $[-B, +B]$ of control is convex, and the initial and final configurations X_0 and X_f are fixed. Finally, one can easily check the existence of a constant C such that ${}^t X\, F(X, v) \leq C\,(|X|^2 + 1)$ for all $t \in [0, T]$, $X \in \mathbf{R}^2 \times S^1 \times \mathbf{R}$, $v \in [-B, +B]$.

Fillipov's theorem then asserts the existence of some $T^* > 0$ and of an optimal control $v^*(t)$ which is a measurable (thus locally integrable) function which satisfies (31) on $[0, T^*]$. The solution of (30) for $v = v^*$ is a path from X_0 to X_f which minimizes cost (32) under constraint (31).

6.2 Necessary conditions for a solution to be optimal

Pontryagin's Maximum Principle We are going to apply Pontryagin's Maximum Principle in order to obtain necessary conditions for a solution to be optimal (i.e. a measurable control v and a trajectory X) minimizing cost (32).

Let us denote by Ψ, ${}^t\Psi = (\psi_1, \psi_2, \psi_3, \psi_4)$, the adjoint state associated to X. For this minimum time problem, the Hamiltonian H is defined for every $t \in [0, T]$ by

$$H(\Psi(t), X(t), v(t)) \; = < \Psi(t), F(X(t), v(t)) >$$

This yields in the case of system (30):

$$H(\Psi(t), X(t), v(t)) = \psi_1(t)\cos\theta(t) + \psi_2(t)\sin\theta(t) + \psi_3(t)\kappa(t) + \psi_4(t)v(t). \tag{33}$$

The adjoint state Ψ is defined on $[0, T]$ as a solution to the adjoint system $\dot{\Psi} = -\frac{\partial H}{\partial X}$, which is here:

$$\dot{\Psi}(t) = \begin{cases} \dot{\psi}_1(t) = 0 \;\; \Rightarrow \psi_1(t) = \psi_1 \\ \dot{\psi}_2(t) = 0 \;\; \Rightarrow \psi_2(t) = \psi_2 \\ \dot{\psi}_3(t) = \psi_1(t)\,\sin\theta(t) - \psi_2(t)\,\cos\theta(t) = \psi_1\dot{y}(t) - \psi_2\dot{x}(t) \\ \dot{\psi}_4(t) = -\psi_3(t)\,. \end{cases} \tag{34}$$

Therefore, as ψ_1 and ψ_2 are constant on $[0, T]$ there exists $\lambda \geq 0$ and $\phi \in [0, 2\pi[$ such that, $\forall t \in [0, T]$:

$$\begin{cases} \psi_1(t) \equiv \psi_1 = \lambda\,\cos\phi \\ \psi_2(t) \equiv \psi_2 = \lambda\,\sin\phi \\ \dot{\psi}_3(t) = \lambda\,\sin(\theta(t) - \phi) \\ \dot{\psi}_4(t) = -\psi_3(t)\,. \end{cases} \tag{35}$$

The Hamiltonian (33) can now be written as:

$$H(\Psi, X, v) = \lambda \cos(\theta - \phi) + \psi_3 \kappa + \psi_4 v. \tag{36}$$

Now, according to theorem 3, a necessary condition for $X(T)$ to be an extremal trajectory for the minimum-time problem is that $\Psi(t)$ define a nonzero absolutely continuous function such that $\forall t \in [0, T]$:

$$H(\Psi(t), X(t), v(t)) = \max_{u \in [-B, +B]} H(\Psi(t), X(t), u(t)) = -\psi_0. \tag{37}$$

where $\psi_0 \leq 0$ is a constant.

Characterization of extremal arcs From equation (37) we deduce that:

$$\psi_4(t)\, v(t) \geq 0 \text{ for almost every } t \in [0, T]\,. \tag{38}$$

As X belongs to class $\mathcal{C}$, on each open C^3 portion of the trajectory, $v(t) = \pm B$ with the sign of ψ_4 if $\psi_4(t) \neq 0$ or, otherwise, that $\frac{\partial H}{\partial v} = \psi_4(t) = 0$. If $\psi_4(t) \equiv 0$ over some interval $[t_1, t_2] \subset [0, T]$, (35) implies that $\psi_3(t) \equiv 0$ and $\dot{\psi}_3(t) \equiv 0$. As θ is continuous and $\lambda \neq 0$ (otherwise $\psi_1 = \psi_2 = \psi_3 = 0$ and therefore $\psi_0 = 0$ which is not possible), it follows that $\theta(t) \equiv \phi \pmod{\pi}$. Of course then, $\kappa \equiv v \equiv 0$ on $[t_1, t_2]$. Hence, on each open C^3 portion of the path, $v(t) \in \{-B, +B, 0\}$, and since v has to be continuous on such a portion, it is of one of the three kinds:

1. Cl^+: $v(t) \equiv B,\ \psi_4(t) > 0$
2. Cl^-: $v(t) \equiv -B,\ \psi_4(t) < 0$
3. S: $v(t) \equiv 0,\ \psi_4(t) \equiv 0$

Arcs $\mathrm{Cl}^{\pm}$ are finite portions of *clothoids*. A clothoid[6] (see figure (27)), also known as a "Cornu spiral", is a curve along which the curvature κ depends linearly on the arc length (here equal to t) and varies continuously from $-\infty$ to $+\infty$. Hence, all clothoids Cl^+ (where $v(t) = B$) are translated and rotated copies of a unique clothoid Γ while all clothoids Cl^- (where $v(t) = -B$) are translated, rotated and reflected copies of Γ. Clothoids Cl^+ will be called *direct* clothoids and clothoids Cl^- will be called *indirect* clothoids. The canonical clothoid Γ is chosen as the one defined by the following equations:

$$x(t) = \int_0^t \cos(\frac{B}{2}\tau^2) d\tau$$
$$y(t) = \int_0^t \sin(\frac{B}{2}\tau^2) d\tau\,.$$

[6] More details about clothoiods are given in the next section

Arcs S are line segments, all with the same orientation $\phi \pmod{\pi}$.
From the above discussion, we have:

Proposition 1. Any extremal path in class $\mathcal{C}$ is the C^2 concatenation of line segments (with the same orientation) and of arcs of clothoids (with $\dot{\kappa} = \pm B$), all of finite length. The control function v is constant on each piece: $v = B$ on a direct clothoid Cl^+, $-B$ on an indirect one Cl^-, and 0 on a line segment S.

In the sequel, we denote by "Cl" an arc of clothoid, by "S" an open line segment, and by "." a switching point. "Cl_μ" will further specify, when necessary, the length μ of the arc.

In order to characterize the extremal paths, and, among them, the shortest ones, we consider the following problem: *how are these arcs Cl and S arranged together along an extremal trajectory of class $\mathcal{C}$?*
We provide in the next section a partial answer to this question.

Concatenation of arcs

Lemma 25. $\psi_4 = 0$ at any switching point (Cl.Cl, Cl.S or S.Cl).

Proof: That $\psi_4 = 0$ at a switching point Cl.S or S.Cl follows from the fact that $\psi_4 \equiv 0$ on S and that ψ_4 is continuous. At a switching point Cl.Cl, the sign of v changes and, by (38), also the sign of ψ_4. □

Lemma 26. If $\lambda = 0$, the extremal path consists of one or two arcs and is of type Cl or Cl.Cl.

Proof: If $\lambda = 0$, ψ_3 is constant on $[0, T]$ by (35). If $\psi_3 = 0$, ψ_4 is constant on $[0, T]$ by (35). Moreover, ψ_4 cannot be identically 0, since, otherwise, $(\Psi, \psi_0) \equiv (0, 0)$, which contradicts the necessary conditions of PMP. Hence, it follows from Lemma 25 that the extremal path cannot contain a line segment nor a switching point and thus reduces to a single arc Cl.

If $\psi_3 \neq 0$, $\psi_4(t)$ is a linear function of t by (35) and then vanishes at most at one isolated point. Hence the extremal path is of type Cl or Cl.Cl, by Lemma 25. □

Note that such paths are not *generic*: from any given initial configuration X_0 in $\mathbf{R}^2 \times S^1 \times \mathbf{R}$, the set of final configurations $\{X_f\}$ one can reach through such paths is only 1 or 2-dimensional.

Lemma 27. If an extremal path contains a line segment S, $\lambda = -\psi_0 > 0$.

Proof: along a line segment $\psi_4 \equiv \psi_3 \equiv 0$ and $\theta \equiv \phi \pmod{\pi}$. Hence, $H \equiv \varepsilon\lambda = -\psi_0 \geq 0$, with $\varepsilon = \pm 1$. As $\psi_0 \leq 0$ and $\lambda > 0$ (from Lemma 26), we must have $\varepsilon = +1$ and $\lambda = -\psi_0$. □

From the proof of lemma 27, $\varepsilon = \cos(\theta - \phi) = +1$ on S, and we have:

Corollary 1. Along a line segment S, $\theta \equiv \phi \pmod{2\pi}$.

Lemma 28. $\psi_3 - \psi_1\, y + \psi_2\, x$ is constant along any extremal path. If $\lambda > 0$, for any given $c \in \mathbf{R}$, all the points of an extremal path where $\psi_3 = c$ lie on the same straight line D_c, of direction $\phi \pmod{\pi}$.

Proof: $\dot{\psi_3} = \psi_1\, \dot{y} - \psi_2\, \dot{x}$ from (34), and ψ_1 and ψ_2 are constant. Thus there exists a constant c_0 such that $\psi_1 y - \psi_2 x = \psi_3 + c_0$, which proves the first part of the lemma. If $\lambda \neq 0$, ψ_1 and ψ_2 cannot be both equal to 0 and $\psi_1 y - \psi_2 x = c + c_0$ is the equation of a line of direction $\theta = \phi \pmod{\pi}$. □

As a consequence, we have:

Corollary 2. Any line segment S of an extremal path is contained in D_0 and is run with $\theta \equiv \phi \pmod{2\,\pi}$.

Proof: since $\psi_3 \equiv 0$ on S, it follows from Lemma 28 that S is contained in the line D_0 of direction ϕ. By Corollary 1, $\theta \equiv \phi \pmod{2\,\pi}$. □

Lemma 29. If $\lambda > 0$, each open arc of clothoid Cl_μ with $\mu > 0$ of an extremal path, except possibly the initial and the final ones, intersects D_0 at least once.

Proof: let Cl_μ be an arc of length μ of an extremal path which is not the initial nor the final arc. Both endpoints of such an intermediate arc are switching points. Let $]t_1, t_2[$ denote the time interval during which this intermediate arc Cl_μ is run. By Lemma 25, $\psi_4(t_1) = \psi_4(t_2) = 0$. As $t_2 - t_1 = \mu > 0$, there exists at least one $t \in]t_1, t_2[$, say t_3, such that $\dot{\psi}_4(t_3) = 0$ and thus, from (35), $\psi_3(t_3) = 0$. Finally, it follows from Lemma 28 that $M(t_3)$ belongs to D_0. □

Observe that the hypothesis $\lambda > 0$ along an extremal path is true as soon as it contains either a line segment (Lemma 27) or more than only two arcs of clothoid (Lemma 26).

Lemma 30. An extremal path contains no portion of type S.Cl_μ.Cl or of symmetric type Cl.Cl_μ.S with $\mu > 0$.

Proof: assume that there exists such a portion S.Cl_μ.Cl and let $]t_1, t_2[$ denote the time interval during which Cl_μ is run, with $t_2 - t_1 = \mu > 0$. From Lemma 2, S $\subset D_0$, and since the variables (x, y, θ, κ) are continuous on $[t_1, t_2]$, Cl_μ is tangent to D_0 at $M(t_1)$ and $\kappa(t_1) = 0$. Hence, $M(t_1)$ is the inflection point of the clothoid supporting Cl_μ and D_0 is the tangent to the clothoid at $M(t_1)$. This implies that $\mathrm{Cl}_\mu \setminus \{M(t_1)\}$ is entirely contained in an open half-plane delimited by D_0, see figure (27), which contradicts Lemma 29. □

The last lemma is in fact superseded by the following one, due to H.J. Sussmann.

Lemma 31. An extremal path contains no portion of type S.Cl_μ (or Cl_μ.S) with $\mu > 0$.

Proof: assume that there is a portion of type $\mathrm{S.Cl}_\mu$, with $\mu > 0$, in an extremal trajectory and let t_1 be the switching time between S and Cl_μ. From (35) and (36) we obtain the following expressions of the four first derivatives of ψ_4 (valid on S as well as on Cl_μ):

$$\begin{cases} \ddot{\psi}_4 = -\lambda \sin(\theta - \phi) \\ \dddot{\psi}_4 = -\lambda \kappa \cos(\theta - \phi) \\ \ddddot{\psi}_4 = \lambda \kappa^2 \sin(\theta - \phi) + (\psi_3 \kappa + \psi_4 v + \psi_0) v \,. \end{cases}$$

Hence, the adjoint variable ψ_4 is of class C^3 in the neighbourhood of t_1. Moreover, on S, $\psi_4 = \dot{\psi}_4 = 0$, $\theta \equiv \phi \pmod{2\pi}$, $\psi_3 = 0$, $\kappa = 0$. From the above equations, we also have $\ddot{\psi}_4 = \dddot{\psi}_4 = 0$ on S, and, by continuity, at t_1. Moreover, $\ddddot{\psi}_4\,(t_1) = \psi_0\, v$. Thus, there exists an ε, $0 < \varepsilon \leq \mu$, such that for $t \in [t_1, t_1 + \varepsilon[$ we have:

$$\psi_4(t) = \psi_0\, v(t)\, \frac{(t - t_1)^4}{4!} + o((t - t_1)^5) \,.$$

Now, from Lemma 27, $\psi_0 < 0$, so that ψ_4 and v have opposite signs on $[t_1, t_1 + \varepsilon[$ which contradicts (38). □

A consequence of Lemmas 30 and 31 is the following proposition:

Proposition 2. If an extremal path of class $\mathcal{C}$ contains but is not reduced to a line segment, then it contains an infinite number of concatenated clothoid arcs which accumulate towards each endpoint of the segment which is a switching point.

Proposition 2 together with the fact that a clothoid Cl is contained in a ball of bounded diameter D_{Cl} (depending on the parameter B) implies the following:

Proposition 3. The number n of C^3 pieces contained in a generic extremal path cannot be uniformly bounded from above (with respect to X_0, X_f). However, if $d(M_0, M_f)$ denotes the Euclidean distance in the plane between M_0 and M_f, we have that:

$$n \geq \frac{d(M_0, M_f)}{D_{Cl}} \,.$$

Proof: either the shortest path contains (and is generically not reduced to) a line segment, and Proposition 2 implies that there are infinitely many arcs of clothoid, or it is made only with arcs of clothoid, the number of which clearly depends on (and increases with) the distance between X_0 and X_f. The bound from below is obvious. □

6.3 Conclusion

Note that it is not clear whether or not extremal trajectories described in Proposition 2, and, among them, the optimal ones, belongs to class $\mathcal{C}$: indeed, the set of switching points on an optimal trajectory (points where the control v is undefined) might even be uncountable. Moreover, we don't know yet if the statement of this proposition remains true without the assumption that the path contains a line segment.

However, Propositions 2 and 3 already indicate that the optimal control associated to problem (30), (31), (32) has a complex behavior. Contrarily to what occurs for Dubins or Reeds and Shepp problems, for which every optimal trajectory contains at most a prescribed (finite) number of line segment and arcs of circles, the number of switching points is unbounded here and might be infinite.

6.4 Related works

Lemma 31 is due to H.J. Sussmann who provided a complete study of this problem described as "Markov-Dubins problem with angular acceleration control" [38]. In this paper, the author uses results by Zelikin and Borisov [39] to show that there exist extremals involving infinite chattering.

7 Time-optimal trajectories for Hilare-like mobile robots

The last model we consider is the model of Hilare the robot of LAAS-CNRS whose locomotion system consists of two parallel driven wheels and four slave castors.

Let (x, y) be the coordinates of the reference point located between the driven wheels, and θ the robot's orientation with respect to the $x-$axis. v_r and v_l denote respectively the velocities of the contact point of the right and left driven wheel with the floor. These virtual point velocities are considered as two state variables while their acceleration a_r and a_l constitute the two system inputs. Therefore, a configuration of the robot is a 5-uple (x, y, θ, v_r, v_l). Using d to denote the distance between the driven wheels we get the following dynamic representation:

$$\begin{pmatrix} \dot{x} \\ \dot{y} \\ \dot{\theta} \\ \dot{v}_r \\ \dot{v}_l \end{pmatrix} = \begin{pmatrix} \frac{v_r+v_l}{2}\cos\theta \\ \frac{v_r+v_l}{2}\sin\theta \\ \frac{v_r-v_l}{d} \\ 0 \\ 0 \end{pmatrix} + \begin{pmatrix} 0 \\ 0 \\ 0 \\ 1 \\ 0 \end{pmatrix} a_r + \begin{pmatrix} 0 \\ 0 \\ 0 \\ 0 \\ 1 \end{pmatrix} a_l \qquad (39)$$

Each wheel is driven by an independent motor and the power limitation is expressed by the constraint: $a_r, a_l \in [-a, a], a > 0$. For this model there is no curvature constraint and the robot can turn about its reference point.

We consider the problem of characterizing minimum-time trajectories linking any pair of configurations where the robot is at rest i.e verifying $v_r = v_l = 0$.

This problem has been initially studied by Jacobs *et al* [25]. After having shown that the system is controllable, the authors have proven that minimum-time trajectories are necessarily made up with bang-bang pieces. To illustrate the reasoning of their proof let us suppose that the first control a_r is singular while the second control a_l is bang-bang.

For this minimum-time problem, denoting by $\psi = (\psi_1, \psi_2, \psi_3, \psi_4, \psi_5)^T$ the adjoint vector, the Hamiltonian corresponding to system (39) is:

$$H = \psi_1 \frac{v_r + v_l}{2} \cos\theta + \psi_2 \frac{v_r + v_l}{2} \sin\theta + \psi_3 \frac{v_r - v_l}{2} + \psi_4 \, a_r + \psi_5 \, a_l$$

As we suppose a_r to be singular, the corresponding switching function ψ_4 vanishes over a nonzero interval of time. From the adjoint equation we get:

$$\dot{\psi}_4 = -\frac{\partial H}{\partial v_r} = \frac{\psi_1}{2} \cos\theta + \frac{\psi_2}{2} \sin\theta + \frac{\psi_3}{d} = 0$$

and therefore,

$$\psi_3 = -\frac{d}{2}(\psi_1 \cos\theta + \psi_2 \sin\theta)$$

Taking the derivative of ψ_3 and replacing $\dot{\theta}$ by its expression given by (39) we get:

$$\dot{\psi}_3 = (\psi_1 \sin\theta - \psi_2 \cos\theta)(\frac{v_r - v_l)}{2}) \tag{40}$$

The expression of $\dot{\psi}_3$ can also be deduced directly from the adjoint equation:

$$\dot{\psi}_3 = -\frac{\partial H}{\partial \theta} = (\psi_1 \sin\theta - \psi_2 \cos\theta)(\frac{v_r + v_l)}{2}) \tag{41}$$

Equating (40) and (41) we deduce that

1. either $v_2 \equiv 0$
2. either $\psi_1 \sin\theta - \psi_2 \cos\theta = 0$

As a_l is supposed to be bang-bang the first case leads to a contradiction. On the other hand, as $\frac{\partial H}{\partial x} = \frac{\partial H}{\partial y} = 0$, we deduce from the adjoint equation that ψ_1 and ψ_2 are constant. Thus, in the second case, the car is moving on a straight line, but a necessary condition for such a motion to be time-optimal is that the acceleration of wheels be both maximal or both minimal, and therefore correspond to bang-bang control.

Using the same reasoning in the case that a_l is singular and a_r regular, or in the case that both control are singular, one can prove that extremal controls are necessarily bang-bang.

Therefore, optimal trajectories are obtained for $|a_r| = |a_l| = a$; these extremal curves are of two types.

- $a_r = -a_l = \pm a$
  In this case the robot's linear acceleration is null: $\dot{v}(t) = \frac{1}{2}(\dot{v}_d + \dot{v}_g) = 0$. $v(t)$ is constant equal to v_0, therefore the curvilinear abscissa $s(t) = v_0 t$. $\dot{v}_r(t) = \pm a$ while $\dot{v}_l(t) = \mp a$. Integrating we get: $v_r(t) = \pm at + v_{r0}$, $v_l(t) = \mp at + v_{l0}$ and $\omega(t) = \dot{\theta}(t) = \pm\frac{2a}{d}t + \omega_0$. The curvature κ is then:

$$\kappa(t) = \frac{\pm\frac{2a}{d}t + \omega_0}{v_0} = \pm k_c s(t) + \frac{\omega_0}{v_0} \tag{42}$$

  where $k_c = \frac{2a}{dv_0^2}$. In the $(x, y)-$plane, the curve is a clothoid with characteristic constant k_c. When $x_0 = y_0 = \omega_0 = \theta_0$ the curve is expressed by the following parametric expression in terms of Fresnel sine and cosine.

$$\begin{cases} x(t) = sign(v_0)\sqrt{\frac{\pi}{k_c}}\int_0^{\sqrt{\frac{2a}{d\pi}}t} \cos(\frac{\pi}{2}\tau^2)d\tau \\ y(t) = sign(v_0 a_r)\sqrt{\frac{\pi}{k_c}}\int_0^{\sqrt{\frac{2a}{d\pi}}t} \sin(\frac{\pi}{2}\tau^2)d\tau \end{cases} \tag{43}$$

  Figure (27) shows a clothoid obtained for $a_r = -a_l = a$. The part located above the $x-$axis describes the robot's motion for $v_0 > 0$, while the part located under the $x-$ axis corresponds to $v_0 < 0$. A curve symmetric with respect to the $x-$axis is obtained for $a_r < 0$.

  Remark 12. *When $v_0 = 0$ the curve is reduced to a pure rotation about the origin.*

- $a_r = a_l = \pm a$
  In this case the angular velocity is null: $\dot{\omega}(t) = \frac{1}{d}(\dot{v}_r(t) - \dot{v}_l(t)) = 0$. Therefore $\omega(t) = \omega_0$, and $\theta(t) = \omega_0 t + \theta_0$. The linear acceleration is $\dot{v}(t) = sign(a_r)a$, thus $v(t) = sign(a_r)at + v_0$. The curvature radius $\rho(t)$ is given by:

$$\rho(t) = \frac{v(t)}{\omega(t)} = sign(a_r)k_a(\theta(t) - \theta_0) + \frac{v_0}{\omega_0} \tag{44}$$

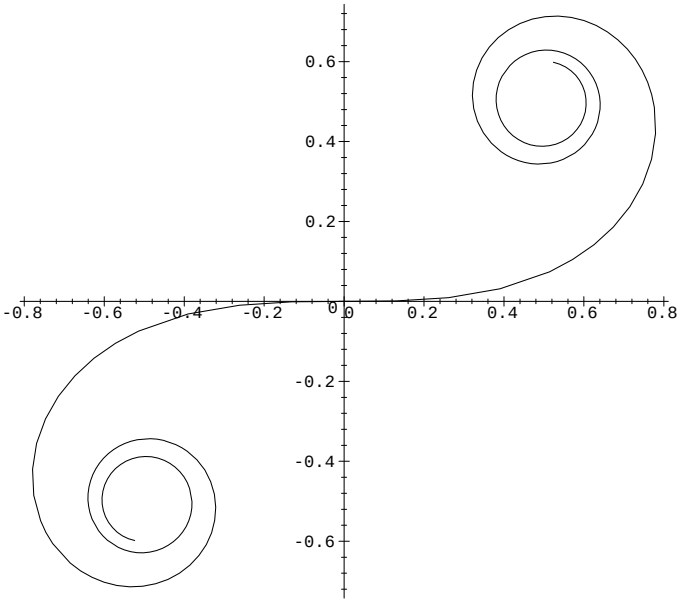

Fig. 27. clothoid obtained for $a_r = -a_l = a$

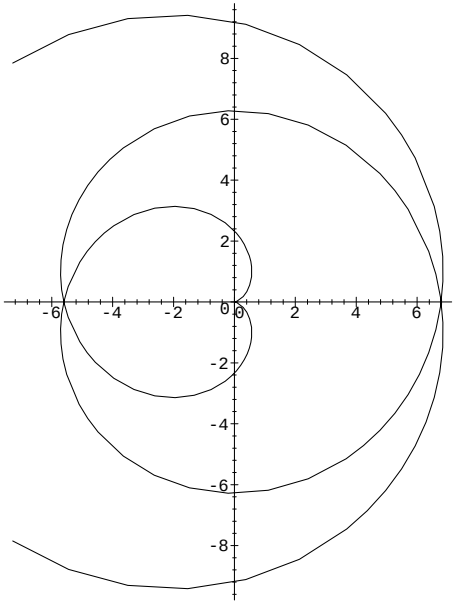

Fig. 28. Involute of circle obtained for $a_r = a_l = a$

where $k_a = \frac{a}{\omega_0^2}$. In the $(x, y)-$plane the curve is an involute of a circle[7] whose characteristic constant is k_a. When $x_0 = y_0 = v_0 = \theta_0$ the curve is expressed by the following parametric expression:

$$\begin{cases} x(t) = sign(a_r)k_a(\cos(\omega_0 t) + \omega_0 t \sin(\omega_0 t) - 1) \\ y(t) = sign(a_r)k_a(\sin(\omega_0 t) - \omega_0 t \cos(\omega_0 t)) \end{cases} \tag{45}$$

Figure (28) represents an involute of a circle obtained for $a_r = a_l = a$. The robot turns in the counterclockwise direction when $\omega_0 > 0$ and in the clockwise direction when $\omega < 0$. For $a_r < 0$ the resulting curve is symmetric with respect to the origin.

Remark 13. *When $\omega_0 = 0$, the curve is a line.*

This description achieves the local characterization of extremal curves. Optimal trajectories are made up with pieces of clothoids and involute of circles. The question is now to determine how many control switches occur along an optimal trajectory and how to determine the switching times. This difficult problem has motivated several research works.

A first work by Reister and Pin [30] was based on the conjecture that optimal paths contain at most four control switches. Using an interesting time parameterization they presented a numerical study of bang-bang trajectories containing only five elementary pieces. By computing the set of accessible configurations in fixed time they tried to state that trajectories containing more than five pieces are not optimal. Unfortunately this numerical analysis could not provide a mathematical proof to bound the number of control switches.

More recently, the work by Renaud and Fourquet [32] has invalidated the conjecture by Reister and Pin, showing that certain configurations of the space could not be reached by extremal trajectories containing only five elementary pieces. Furthermore, they pointed out the existence of extremal solutions allowing to reach these configurations and containing more than four switches.

To our knowledge this work constitutes the last contribution to the problem. Therefore, to date, there does not exist any result allowing to bound the number of control switches along an optimal trajectory. It is then not possible at this stage to try to characterize a sufficient family as we did at section (4). In fact, the very first question we need to answer is to determine whether the number of switches is finite or not.

In spite of solving the minimum-time problem the local description of extremal curves can be used to deduce interesting geometric properties for path planning.

[7] The involute of a circle is the curve described by the end of a thread as it is unwound from a stationary spool.

- Equation (42) show that clothoid allow to link smoothly curves with zero curvature (lines) and curves with nonzero curvature (arcs of circle).
- Equation (44) show that involutes of circle can link smoothly curves with infinite curvature (turn about) and curves with nonzero curvature. In particular, following this curve the robot can make a cusps while keeping a nonzero angular velocity.

This result has been used by Fleury *et al* [17] to design primitives for smoothing mobile robots' trajectories. In this work several sub-optimal strategies are proposed to smooth broken lines trajectories in a cluttered environment.

8 Conclusions

The study of these four problems corresponding to different models of wheeled robots illustrates the strengths and weaknesses of the use of optimal control for path planning.

By constructing a shortest paths synthesis for the models of Reeds and shepp and the model of Dubins, we have definitely solved the path planning problem for a car-like robot moving in a plane free of obstacles. Obviously, as the vehicle is supposed to move at a constant speed along arcs of circle and line segments this result does not constitute a real feedback control for the robot. However, it constitutes a canonical way to determine a path, for linking any two configurations, upon which path following techniques can be developed.

Furthermore, from this construction, it has been possible to determine a distance function providing a topological analysis of the path planning problem. In particular, for the Reeds and Shepp problem, we have proven that the distance induced by the shortest path is Lipschitz equivalent to a sub-Riemannian metric. Such a metric constitutes a very useful tool to compute the distance between the robot and its environment.

However, whereas optimal control may provide a very complete result for a small number of systems, the characterization of optimal path is in general incomplete. This is illustrated by the last two problems. In such cases, the local characterization of extremals can be used to determine suboptimal strategies for planning.

Beyond solving the path planing problem, this study has permitted to get very interesting results.

First, we have shown the existence of symmetry properties common to the different models of wheeled robots. On this basis, by constructing the set of reachable configuration for the model of Reeds and Shepp and for the model of Dubins, we have shown the existence of several propagating wave fronts intersecting each other. From this, we have proven the insufficiency of the local

information provided by PMP and the need to be compare the cost of trajectories corresponding to different wave fronts, by means of global arguments. Using this reasoning we have completely solved the problem of Reeds and Shepp as well as the problem of Dubins.

On the other hand, by showing that the synthesis constructed for the Reeds and Shepp problem verifies the required regularity conditions we have found another proof to confirm this result *a posteriori* by applying Boltianskii's sufficient optimality conditions. Though this theorem allows to prove very strong results in a very simple way, we have shown the narrowness of its application area by considering the neighbouring example of Dubins for which the regularity conditions no longer apply because of the discontinuity of path length.

The last two examples illustrate the difficulty very often encountered in studying of optimal control problems. First, the adjoint equations are seldom integrable making only possible the local characterization of optimal paths. The search for switching times is then a very difficult problem. Furthermore, as we have seen in studying the problem of Dubins with inertial control, it is possible to face Fuller-like phenomenon though the solution could seem to be a priori intuitively simple.

References

1. L.D Berkovitz, "Optimal Control Theory," *Springer-Verlag,* New York, 1974.
2. J.D. Boissonnat, A. Cerezo and J. Leblond, "Shortest paths of bounded curvature in the plane," in *IEEE Int. Conf. on Robotics and Automation*, Nice, France, 1992.
3. J.D. Boissonnat, A. Cerezo and J. Leblond, "A Note on Shortest Paths in the Plane Subject to a Constraint on the Derivative of the Curvature," *INRIA Report No 2160, january 1994*
4. V.G. Boltyanskii, " Sufficient conditions for optimality and the justification of the dynamic programming method," *J.Siam Control,* vol 4, No 2, 1966.
5. R.W Brockett, " Control Theory and Singular Riemannian Geometry," *New Direction in Applied mathematics* (P.J. Hilton and G.S. Young, eds), Springer, pp 11-27, Berlin, 1981.
6. I.N. Bronhstein and K.A. Semendyayev, "A guide-book to Mathematics for technologists and engineers," *Pergamon Press,* 1964.
7. P. Brunovsky, "Every normal linear system has a regular synthesis," *J. Diff. Equations,* 28, pp 81-100, 1978.
8. P. Brunovsky, "Existence of regular synthesis for general problems," *J. Diff. Equations* 38 pp 317-343, 1980.
9. X-N. Bui, P. Soures, J-D. Boissonnat and J-P Laumond, "The Shortest Path Synthesis for Non-Holonomic Robots Moving Forwards", *INRIA Report N^o 2153*, january 1994.
10. X-N. Bui, P. Souères, J-D. Boissonnat and J-P Laumond, "Shortest Path Synthesis for Dubins Nonholonomic Robot", *IEEE Int. Conf. on Robotics and Automation,* San Diego California, 1994.
11. X-N. Bui, "Planification de trajectoires pour un robot polygonal non-holonome dans un environement polygonal," *PhD Thesis, Ecole Nationale Supérieure des Mines de Paris, France* 1994.
12. S.S Cairns, "On the triangulation of regular loci", *Ann. of Math., 35, pp 579-587* (1934)
13. L. Cesari " Optimization, theory and applications," *Springer-Verlag,* New york, 1983.
14. R. Chatila, "Mobile robot navigation: space modeling and decisional processes," in *Robotics Research : The Third International Symposium* (O. Faugeras and G. Giralt, eds.), MIT Press, pp. 373–378, 1986.
15. E.J. Cockayne and G.W.C. Hall, "Plane motion of a particle subject to curvature constraints," *SIAM J. Control,* 13 (1), 1975.
16. L. E. Dubins, "On curves of minimal length with a constraint on average curvature and with prescribed initial and terminal positions and tangents," *American Journal of Mathematics,* Vol. 79, pp. 497–516, 1957.
17. S. Fleury, P. Soures, J-P. Laumond, R. Chatila, " Primitives for Smoothing Mobile Robot Trajectories," *IEEE Transactions on Robotics and Automation* Vol. 11, No 3, June 1995.
18. M. Fliess, J. Levine, Ph. Martin, and P. Rouchon. " Sur les systmes non linaires diffrentiellement plats," *C.R. Acad. Sci Paris,* I-315:619-624, 1992.
19. J-Y.Fourquet "Mouvements en temps minimal pour les robots manipulateurs en tenant compte de leur dynamique non linaire." *PhD Thesis, Universit P.Sabatier* N^o 800, France, 1990.

20. G. Giralt, R. Chatila, and M. Vaisset, "An integrated navigation and motion control system for autonomous multisensory mobile robots," in *Robotics Research : The First International Symposium* (M. Brady and R. P. Paul, eds.), MIT Press, pp. 191–214, 1984.
21. H. Halkin " Mathematical Foundation of System Optimization" in *Topics in Optimization,* edited by G. Leitmann, Academic Press, 1967.
22. P. Hartman. "The highway spiral for combining curves of different radii." *Trans. Amer. Soc. Civil Engin.,* 1957
23. A. Isidori, "Nonlinear Control Systems," (second edition) *Springer-Verlag,* 1989.
24. G. Jacob "Lyndon discretization and exact motion planning," in *European Control Conference,* pp. 1507-1512 Grenoble, France, 1991.
25. P. Jacobs, A Rege and J-P. Laumond, "Non-Holonomic Motion Planning for Hilare-Like Mobile Robots," *Proceedings of the International Symposium on intelligent Robotics,* Bangalore, 1991.
26. J.P. Laumond and P. Souères, "Metric induced by the shortest paths for a car-like mobile robot", in *IEEE IROS'93*, Yokohama, July 1993.
27. C. Lobry, "Controlabilité des systèmes non lineéaires," *outils et modèles mathématiques pour l'automatique, l'analyse des systèmes et le traitement du signal,* 1: pp 187-214, CNRS, 1981.
28. R. Felipe Monroy Pérez, "Non-Euclidian Dubin's problem: A control theoretic approach", *PhD thesis*, Department of Mathematics, University of Toronto, 1995.
29. L.S Pontryagin, V.G. Boltianskii, R.V. Gamkrelidze, and E.F. Mishenko. "The mathematical Theory of Optimal Processes," *Interscience Publishers,* 1962.
30. D.B. Reister and F.G. Pin, "Time-optimal trajectories for mobile robots with two independently driven wheels." *International Journal of Robotics Research, Vol 13, No 1, pp 38-54*, February 1994.
31. J. A. Reeds and R. A. Shepp, "Optimal paths for a car that goes both forwards and backwards, " *Pacific Journal of Mathematics*, 145 (2), 1990.
32. M. Renaud and Jean-Yves Fourquet, "Minimum-time motion of a mobile robot with two independant acceleration-driven wheels," *IEEE International Conference on Robotics and Automation*, Albuquerque, USA, April 1997.
33. P. Souères and J.P. Laumond, " Shortest paths synthesis for a car-like robot" *IEEE Transaction on Automatic Control*, Vol 41, No 5 May 1996.
34. P. Souères, "Comande optimale et robots mobiles non holonomes," *PhD Thesis, Universit'e Paul Sabatier, N° 1554,* France, 1993.
35. P. Souères, " Applying Boltianskii's sufficient optimality conditions to the characterization of shortest paths for the Reeds-Shepp car," *third European Control Conference ECC'95*, Roma, Italia, Sept. 1995.
36. H.J. Sussmann and W. Tang, "Shortest paths for the Reeds-Shepp car : a worked out example of the use of geometric techniques in nonlinear optimal control," *Report SYCON-91-10, Rutgers University,* 1991.
37. H.J. Sussmann, "Shortest 3-dimensional paths with a prescribed curvature bound", *Proc. of the 34th Conference on Decision and Control*, New Orleans, LA - December 1995.
38. H.J. Sussmann, "The Markov-Dubins problem with angular acceleration control", *Proc. of the 36th Conference on Decision and Control*, San Diego, CA - December 1997.

39. M.I. Zelikin and V.F. Borisov, "Theory of Chattering Control, with applications to astronotics, robotics, economics and engineering", *Birkhäuser*, Boston, 1994.